LUPINE PUBLISHERS

Research and Reviews on Healthcare: Open Access Journal

DOI: 10.32474/RRHOAJ.2023.08.000282

ISSN: 2637-6679

Review Article

New Drug Discovery of Anti-Neuropathic Pain agents: Insights in Animal Models

Ashish Kumar Sharma[1]*, Mehvish Bhat[1], Shivam Singh[1], Kartik Gill[1], Mohammad Zaid[1], Junaid Tantray[1], Sanjay Kumar Sahu[2], Rajesh Kumar Sharma[1], Gulshan Rathore[1], Priyanka Chandolia[1], Anjali Shakya[1], Sachin Kumar[1], Divyamol Jose[1], Rashmi Gupta[1], Shobhit Raj[1], Archita Gupta[1], Mithilesh Singh[1], Anurag Mishra[1], Parth Vaibhav[1], Prashant Gupta[1], Nancy Kathuria[1], Ankit Vashist[1], Vipin Yadav[1], Mohit Agarwal[1], Anamika Gupta[1], Sumaiya Kifayat[1], Tsering Yangzom[1], Ravindra Pal Singh[1] and Arun Garg[3]

[1]NIMS Institute of Pharmacy, NIMS University Rajasthan, India

[2]General Manager, Formulation & Development-R&D, Medley Pharmaceuticals Ltd., India

[3]Vice-Chancellor, MVN University, India

***Corresponding author:** Kumar Sharma, Professor, NIMS Institute of Pharmacy, NIMS University Rajasthan, Jaipur, Rajasthan, Pincode-303121, India

Received: June 01, 2023 **Published:** June 14, 2023

Abstract

Understanding pathobiology of neuropathic pain, animal models has been crucial for developing effective therapies for humans. Common complications of their underlying disorders profoundly diminish the quality of life of affected persons. To replicate clinical pain disorders with various origins, a battery of neuropathic pain models has been developed. In this review, methodology, behavioural changes, advantages, and disadvantages of several different animal models of neuropathic pain are examined in depth. Knowledge about chronic pain, underlying brain and peripheral pathogenic pathways utilized for creation of these models. The development of innovative medications for the treatment of neuropathic pain has also resulted from research, and the preclinical knowledge gained from these animal models has progressively been translated into effective pain management in human settings. Since every animal model was created using a different methodology result in typically diverge dramatically with even little variations in methodology. Data from numerous models can be presented and interpreted in the relation management of the specific origin of pain as depicted by each neuropathic pain model. Conclusion: Experimental models of neuropathic pain gives quick summary of most popular animal models, their characteristics, and their significance for new drug discovery for novel anti-neuropathic pain agents.

Keywords: Animal models to screen Drugs for Neuropathic Pain; peripheral neuropathy; central pain; cancer pain; anti-cancer agents; trigeminal neuralgia; HIV, post-herpetic neuralgia

Introduction

A nerve injury may cause "the most horrific of all tortures," according to one description of neuropathic pain [1,2]. Sensory abnormalities such as unpleasant aberrant sensations (dysesthesia), an enhanced reaction to painful stimuli (hyperalgesia), and pain in response to a stimulus that does not typically cause pain are characteristics of neuropathic pain (allodynia) [3]. Patients with cancer, AIDS, long-term diabetes, multiple sclerosis, stroke, lumbar disc syndrome, herpes, traumatic spinal cord injury (SCI), long-term diabetes, and long-term diabetes are commonly seen to experience peripheral neuropathic pain [4]. Other disorders that frequently involve discomfort from peripheral neuropathy include post-thoracotomy, post-herniorrhaphy, post-mastectomy, and post-sternotomy [5]. Pharmacotherapy for neuropathic pain has had very patchy effectiveness, with NSAIDS and opiates and other regularly used painkillers producing little to no response [3]. As a result, there is a great need to investigate cutting-edge therapy approaches. Since most of the stimuli needed to

create neuropathic pain result in irreparable harm, evaluating neuropathic pain in people is difficult. As a result, only humans may employ the stimuli that do not cause permanent injury. Additionally, it is quite challenging to get a big enough human sample size for this kind of study. To better understand the processes behind neuropathic pain and to assess the analgesic potential of novel pharmacotherapies for treating neuropathic pain, there is a need for validated and easily repeatable animal models of neuropathic pain. Allodynia, hyperalgesia, and spontaneous pain should be observable sensory impairments that can be reproduced over an extended period of time in ideal models. Thus, several physio-pathological disorders seen in humans may be replicated by creating sensory defects in animals, allowing for the assessment of pharmacotherapies. Peripheral nerve damage and SCI-induced peripheral and central pain models of neuropathy are only a few examples of the several animal models that have been developed to address the complex causes and, as a result, the numerous symptoms of neuropathy. There are models for pain caused by chemotherapeutic medications, cancer, HIV, post-herpetic neuralgia (PHN), diabetes, and chronic ethanol use, trigeminal neuralgia, and orofacial pain. This review devotes its whole attention to these various and varied animal models of neuropathic pain [1].

Animal models of Neuropathic Pain

Peripheral nerve injury models

The primary complaint in most clinical pain situations is spontaneous pain and responsiveness to noxious or harmless stimuli. The earlier models are therefore only useful for examining acute nociceptive pain and have little use for assessing changes in hypersensitivity related to chronic pain conditions. Wall and colleagues made a substantial addition to our knowledge of the pathophysiological mechanisms behind chronic pain, which is distinct from acute noxious pain, in the 1970s by creating a chronic pain model by injuring a peripheral nerve [6]. As a result, efforts were made to create various animal models of nerve damage as substitutes for human neuropathic pain (Table 1).

Table 1: List of different animal models of neuropathic pain.

S. no.	Name of model	Principle of injury	Species
1	Axotomy (complete sciatic nerve transection)	Complete transection of sciatic nerve	Rats
2	Chronic constriction injury	Four loose ligatures around sciatic nerve	Rats, mice
3	Partial sciatic nerve ligation (Seltzer Model)	Tight ligation of one-third to half of sciatic nerve	Rats, mice
4	Spinal nerve ligation	(i) Tight ligation of L5, L6 spinal nerves	Rats,
		(ii) tight ligation of L7 spinal nerve	Macaca fascicularis
5	Spared nerve injury	Axotomy of tibial and common peroneal nerves	Rats, mice
6	Tibial and sural nerve transection	Axotomy of tibial and sural nerves	Rats
7	Ligation of common peroneal nerve	Ligation of common peroneal nerve	Mice
8	Sciatic cryoneurolysis	Freezing of the sciatic nerve	Rats
9	Caudal trunk resection	Resection of caudal trunk	Rats, mice
10	Sciatic inflammatory neuritis	Injection of zymosan, HMG, TNF-alpha around sciatic nerve	Rats, mice
11	Cuffing-induced sciatic nerve injury	Implantation of polyethylene cuff around sciatic nerve	Rats, mice
12	Photochemical-induced sciatic nerve injury	Thrombosis in small vessels supplying sciatic nerve by photosensitizing dye and laser	Rats, mice
13	Laser-induced sciatic nerve injury	Radiation mediated reduction in blood supply to sciatic nerve	Rats
14	Weight drop or contusive spinal cord injury	Dropping a weight over the exposed spinal cord	Rats, mice
15	Excitotoxic spinal cord injury	Intraspinal injections of excitatory amino acids	Rats, mice
16	Photochemical spinal cord injury	Thrombosis in blood vessels supplying the spinal cord by photosensitizing dye and laser	Rats
17	Spinal hemisection	Laminectomy of T11–T12 segments.	Rats
18	Drugs-induced		
(a)	Anti-cancer agents (vincristine, cisplatin, oxaliplatin, paclitaxel)	Direct injury of drugs to the nerves of peripheral nervous system	Rats, mice, guinea pigs
(b)	Anti-HIV agents (2,3-dideoxycytidine, didanosine)		Rabbits, rats
19	Diabetes-induced neuropathy	Persistent hyperglycemia-induced changes in the nerves	Rats, mice

(a)	Streptozotocin-induced		
(b)	Genetic models		
20	Bone cancer pain models		
(a)	Femur, calcaneus, tibial, humerus bone cancer pain	Inoculation of cancerous cells into respective bones	Rats, mice
(b)	Neuropathic cancer pain	Growing a tumor in vicinity of sciatic nerve	Mice
(c)	Skin cancer pain	Injection of melanoma cells in plantar region of hind paw	Mice
21	HIV-induced neuropathy	Delivery of HIV-1 protein gp120 to sciatic nerve	Rats
22	Post-herpetic neuralgia		
(a)	Varicella Zoster virus	Injection of viral infected cells in the footpad	Rats, mice
(b)	Herpes simplex virus	Depletion of capsaicin-sensitive	
(c)	Non-viral model	Afferents with resiniferotoxin	Rats
23	Chronic ethanol consumption/withdrawal	Administration of ethanol over extended period	Rats
		around 70 days)	
24	Pyridoxine-induced	Administration of high dose pyridoxine for long period	Dogs, rats
25	Trigeminal Neuralgia	Compression of trigeminal ganglion	Rats
		chronic constriction injury to infra-orbital nerve	Rats
26	Orofacial pain	Injection of formalin, carragenan into temporomandibular joints and maxilla	Rats, mice
27	Acrylamide-induced	Administration of acrylamide for prolonged period	Rats
28	Monoiodoacetate model of osteoarthritis	osteoarthritis-related joint degradation	Rats

Axotomy model (complete sciatic nerve transection; neuroma model)

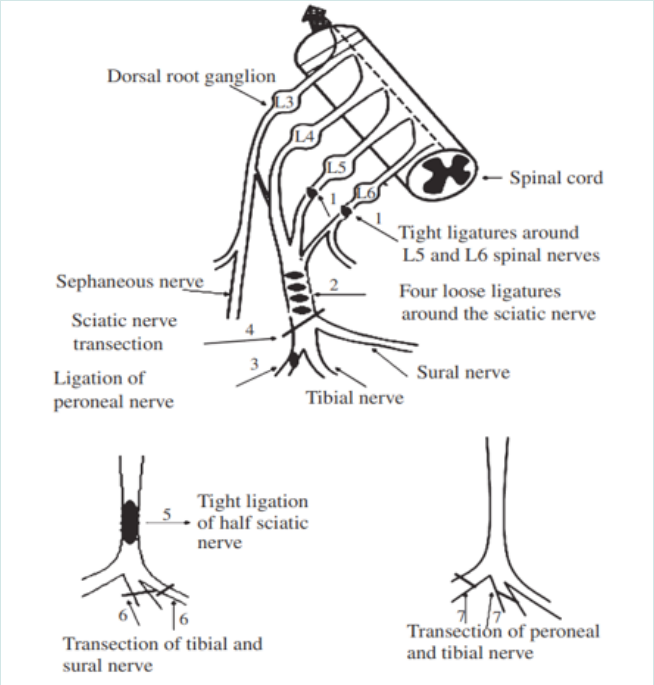

Figure 1: 1 Representation of different peripheral nerve injury models (1) spinal nerve ligation by tightly ligating L5 and L6 spinal nerves, (2) chronic constriction injury by placing four loose ligatures around the sciatic nerve, (3) ligation of common peroneal nerve, (4) axotomy model by sciatic nerve transection, (5) partial sciatic nerve ligation by tight ligation of one-third to half of sciatic nerve, (6) tibial and sural nerve transection model by transection of tibial and sural nerve, (7) spared nerve injury model by transection of peroneal and tibial nerve [10].

It involves completely transecting the sciatic nerve at mid-thigh level and is the first animal model of neuropathic pain [7]. The common sciatic nerve is exposed when the rat is put to sleep in this scenario. The sciatic nerve is firmly bound by nylon suture, proximal to its bifurcation into the tibial and the peroneal divisions, at two points spaced approximately one centimetre apart. The connective tissue that was linked to the sciatic nerve is removed. The remaining 5 mm of the nerve between the ligatures are then removed to prevent the nerve from re-joining owing to regeneration after the nerve has been entirely transacted between the pair of ligatures. To cause complete denervation of the distal hind limb, the nearby saphenous nerve is also injured. Following full nerve transection, a neuroma with regenerating nerves sprouting in all direction's forms at the proximal nerve stump [8,9]. (Figure 1). Anaesthesia dolorosa, or pain in the region in the absence of any sensory input in that location, is produced by the model. In this model, autotomy—self-attack and mutilation of the denervated limb by injured animals—is seen, and it's frequently thought of as a sign of neuropathic pain [11]. The manner and location of neurectomy have an impact on the degree of autotomy [12]. Whether autotomy results from excessive grooming in the absence of sensory feedback or reflects spontaneous pain has been hotly debated [13]. This model's main weakness is that full nerve transections or lesions are very rare in patients and are typically only seen after amputation, as in the case of phantom limb pain. Clinically, the more prevalent types of neuropathies include peripheral nerve partial lesions. Additionally, as animals exhibit severe autotomy in this scenario, ethical issues are also major concerns [14].

Chronic constriction injury (CCI)

One of the most widely used animal models for neuropathic pain, Bennett and Xie created a model of peripheral mononeuropathy in rats by CCI to the sciatic nerve. The common sciatic nerve of the hind paw is exposed at the mid-thigh level after a 3-cm-long blunt incision is done into the skin overlaying the region between the gluteus and biceps femoris muscles under anaesthesia. Near the sciatic trifurcation, roughly 7 mm of nerve is released, and then four or three loose ligatures of 4-0 chromic guts (or 4-0 silk) are wrapped around the sciatic nerve until a fleeting twitch is seen. It is carefully avoided to disrupt the epineural circulation [15,16]. A mouse model that exposes the common sciatic nerve at the level of the mid-thigh and loosely ties it with three ligatures (4/0 chromic silk, Ethicon), spaced approximately 0.5 mm apart, close to the nerve's trifurcation has also been developed [17,18]. This sciatic nerve compression is linked to Wallerian degeneration, localised ischemia, and intraneural edoema. There have been studies on the behavioural indicators of spontaneous pain, including mild to moderate autotomy, guarding, excessive licking, limping of the ipsilateral hind paw, and avoiding putting weight on the injured side. The development of behavioural modifications such as mechanical and thermal hyperalgesia, chemical hyper-reactivity, and cold allodynia has been documented to take place within a week, with the second post-operative week showing the most pain-related behaviours and postural asymmetries [19]. These changes in neuropathic pain have been shown to last for at least 7 weeks following the procedure [15,20]. Histopathological investigations imply that myelinated axons are more damaged than non-myelinated axons, and electrophysiological studies have shown a reduction in nerve conduction velocity [21]. Earlier, it has been proposed that the behavioural alterations seen in this animal following damage are caused by C-fiber sensitization [21]. The sensitivity of both A- and C-fibers because of partial nerve injury has now been shown to contribute to the initiation and maintenance of pain behaviour [22]. It has been noted that the symptoms of unilateral peripheral mononeuropathy caused by the CCI model in rats are like those of complex regional pain syndrome or causalgia in human patients [15] (Figures 2-5). Research on aberrant sensation and spontaneous pain has made considerable use of the CCI model. Additionally, it has helped in the examination of sensory complaints brought on by entrapment neuropathy [23]. However, there has been considerable variance seen in the animals that have sustained chronic constriction damage, which might make quantitative analysis more difficult. These changes might be brought on by variances in the degree of constriction created by the suture knots [25].

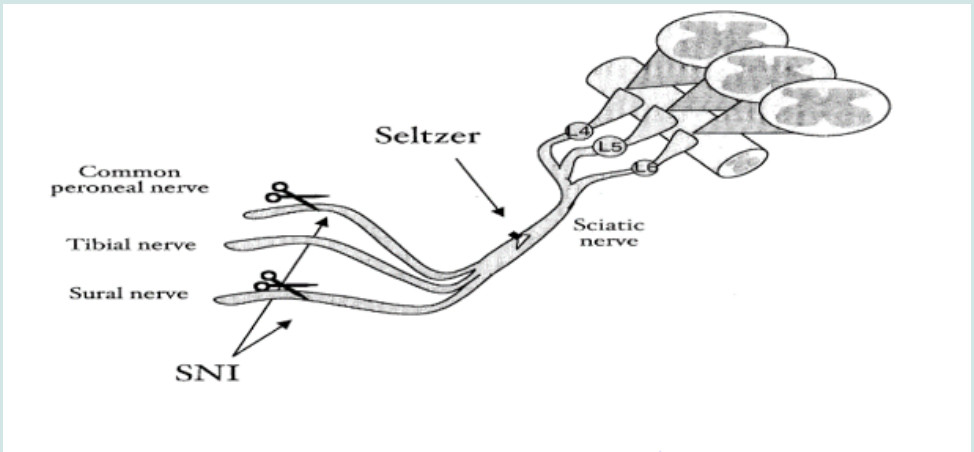

Figure 2: Layout of sciatic nerve and its branches, including manipulations performed for Seltzer and SNI models of neuropathic pain. The common peroneal, tibial, and sural nerves are the 3 distal branches of the sciatic nerve; 2 of the 3 are ligated and cut in the SNI model. Partial tight ligation, or Seltzer model, is performed more proximally and involves tying off 1/3 to 1/2 of the sciatic nerve [42].

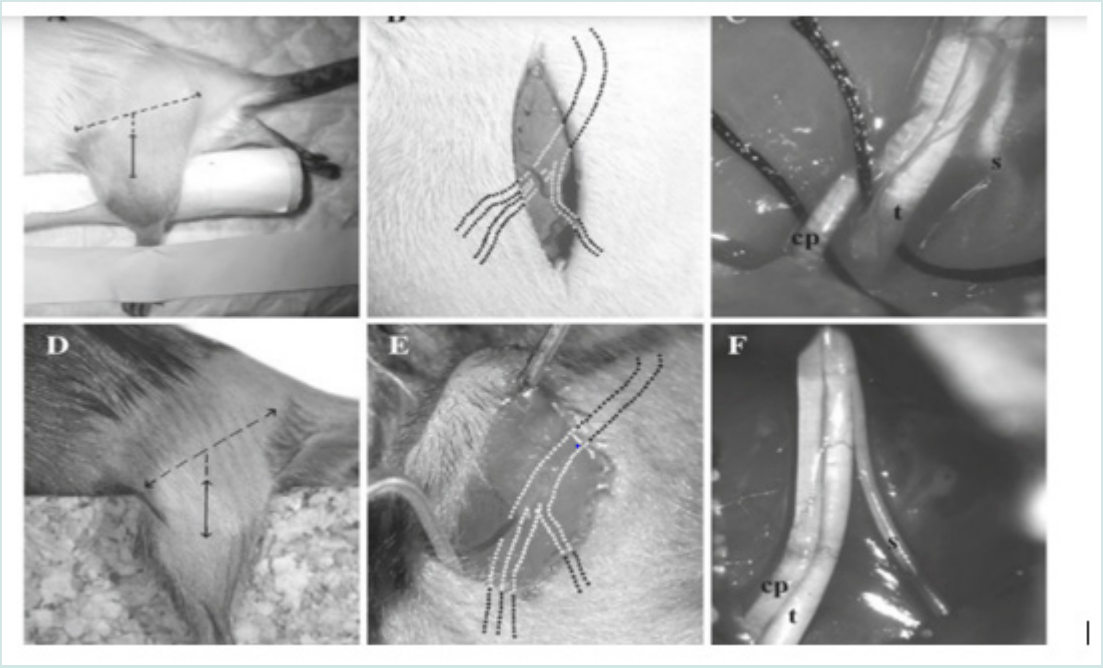

Figure 3: SNI surgery in rats (a – c) and in mice (d – f). The incision (filled double arrow) is made at the middle position of the thigh at a 60° angle from a fictive axe (dashed double arrow) between trochanter major and iliaca cresta (a, d). Dotted lines in (b) and (e) show the position of the sciatic trifurcation underneath the artery genus descendes and biceps femoris. In (c) and (f), the three bared branches of the sciatic nerve are shown (cp common peroneal, t tibial, s sural). The threads aiming at suturing the common peroneal and tibial nerves are shown in (c) before ligation [43].

Figure 4: Panel A demonstrates a rat with abnormal ipsilateral tonic hindpaw toe flexion and hyperalgesia, 6 months after 1/3rd tibial-nerve axotomy. Panel B was photographed from below the mesh floor used for sensory testing. It depicts a rat 4 weeks after left total tibial axotomy with weak left hindpaw adduction and hyperalgesia [53].

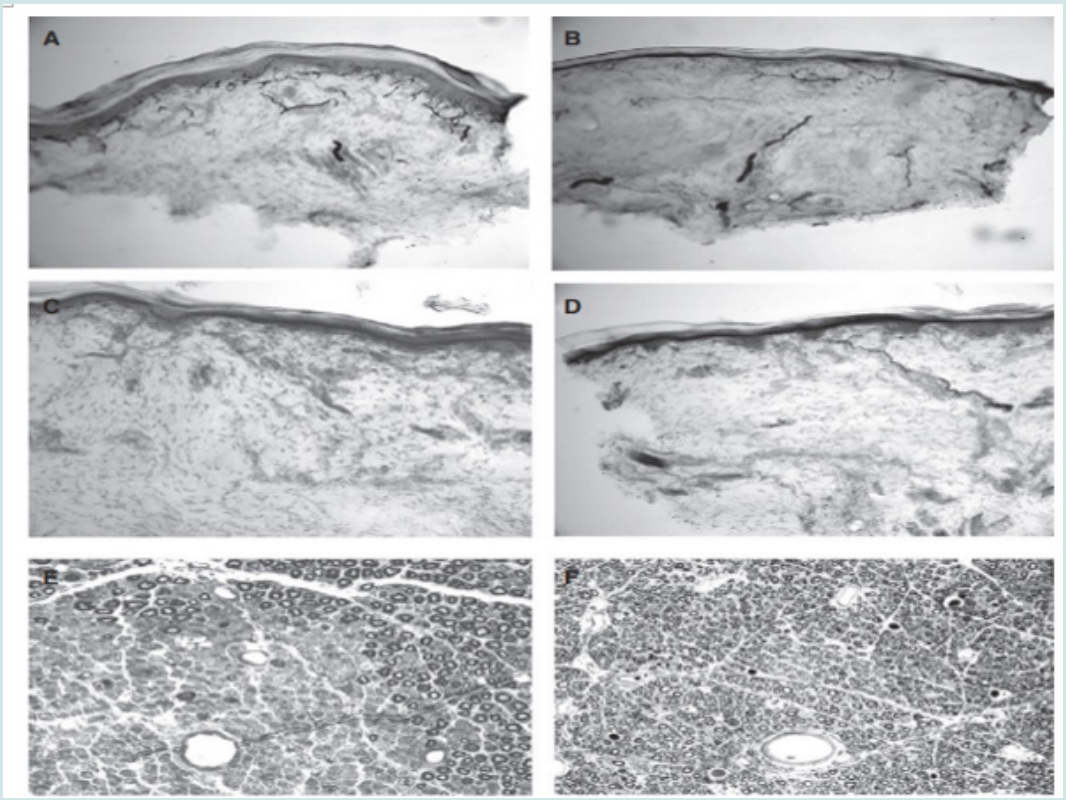

Figure 5: The upper and middle panels are photomicrographs of PGP9.5 immunolabeled, 50-mm thick, vertical sections of tibial-nerve injured hindpaw skin biopsies. Panels A, B, and C were all taken at week 2 postoperatively to show proportional levels of loss of cutaneous innervation after 1/3 axotomy (A), 2/3 axotomy (B), and total axotomy (C). Panel D depicts partial reinnervation of the affected area 6 weeks after total axotomy. The bottom panels depict epoxyembedded, 1 mm sections of injured distal tibial nerve (1% toluidine blue stained). Panel E depicts Wallerian degeneration 2 weeks after 1/3 axotomy. Panel F depicts widespread regeneration (axons with disproportionately thin myelin sheaths) 12 weeks after 2/3rd axotomy [53].

Partial sciatic nerve ligation (PSL/Seltzer model)

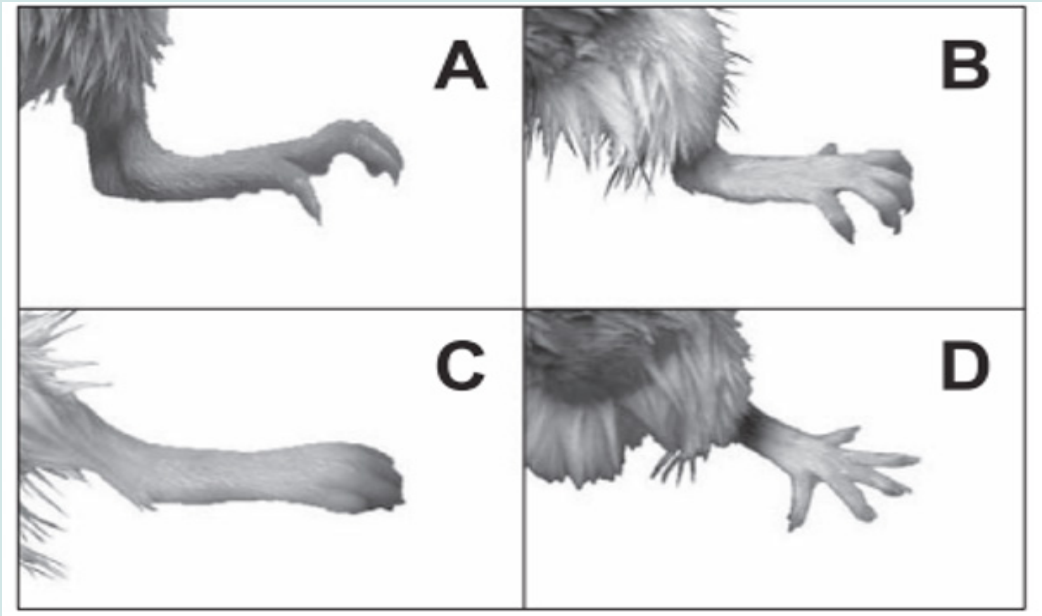

Figure 6: Effects of the ligation of the branches of sciatic nerve on the form of the hind paw. The photos show typical examples one day after sham operation (A) and the tight ligation of sural (B), tibial (C), or common peroneal nerve (D) [55].

One of the more widely used models of neuropathy was created by Seltzer and is based on his work. In this model, the sciatic nerve is exposed at the upper thigh level after shaving the left hind leg of the rat. Just distal to where the posterior biceps semitendinosus nerve splits off, the dorsal third to half of the sciatic nerve is securely ligated with an 8-0 silk suture [26,28]. Paw guarding and licking on the side of the injury are behavioural indications of spontaneous discomfort, according to reports. A week following surgery, most of the behavioural abnormalities, including cold allodynia, chemical hyper-reactivity, and mechanical hyperalgesia, have been seen to occur [20,26,29]. In the first week following surgery, the PSL model mimics sympathetically independent pain (SIP) (Figures 6-10). Later weeks, nevertheless, see it change to sympathetic-dependent pain [27]. Other species, such as mice, have also been used, and it has been observed that a partial sciatic nerve damage in mice results in a similar allodynia and neurochemical plasticity [30]. Depending on the suture material and stresses, pain reactions' intensity and duration might vary greatly [31]. Since partial nerve injury is the primary contributor to causalgiform pain syndromes in people, models of partial nerve injury are pertinent for studying neuropathic pain injury [32,33].

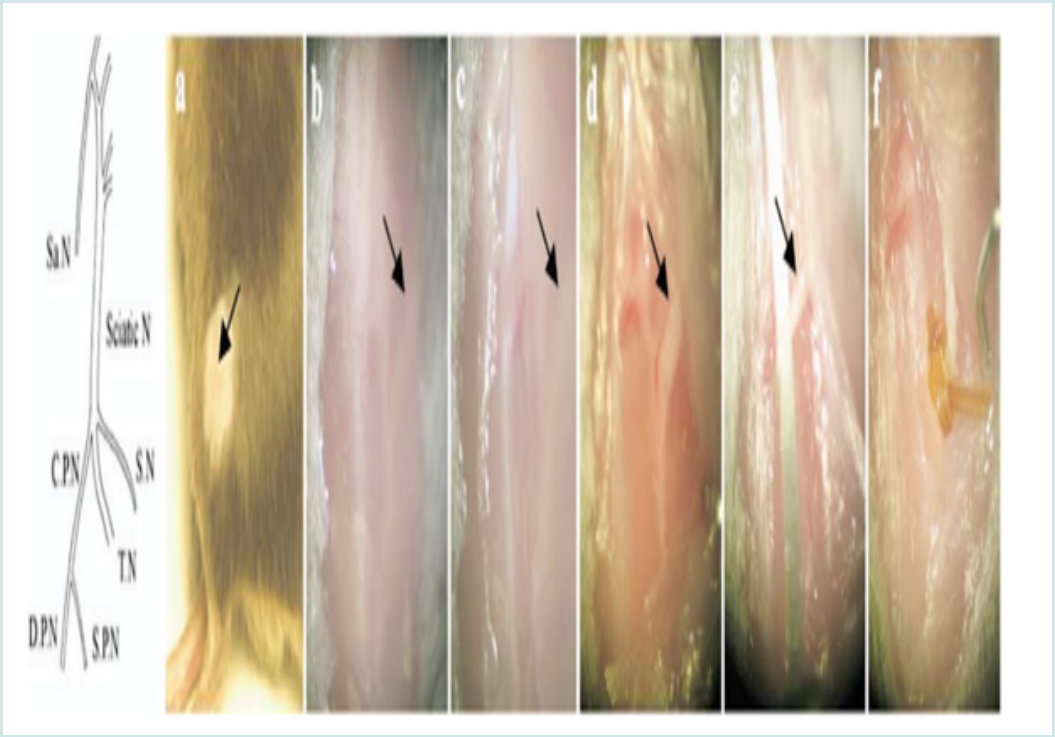

Figure 7: Diagram illustrating the ligation of CPN in mouse. Left panel: Schematic diagram of the left lumbar plexus, sciatic nerve and its branches. Abbreviations: Sa.N, saphenous nerve; C.P.N, common peroneal nerve; D.P.N, deep peroneal nerve; S.N, sural nerve; T.N, tibial nerve; S.P.N, superficial peroneal nerve. (a) Shows the area below and lateral to the knee joint before surgery. The head of the fibula can be palpated at the top of the shaved area. Note the groove between the anterior and posterior compartment of muscles. (b) Shows the view after dissecting the skin. Removal of the thin subcutaneous fascia will make it clearer. Note the white-colored fascia separating the anterior and posterior compartment of muscles. Note that the CPN runs 30 to 45° to the horizontal line and is accompanied by a blood vessel most of the time. The white fascia is lifted up with forceps and a vertical incision is made along the white fascia. (c) Incision along the white fascia separating the anterior and posterior compartment of muscles. Other white structures are tendons or connective tissue fascia. (d) Posterior group of muscles is pulled laterally to view the common peroneal nerve. (e) Suture needle is passed under the nerve. (f) The catgut ligature in place. Only one knot was necessary to maintain the knot in position. Arrows show the common peroneal nerve [56].

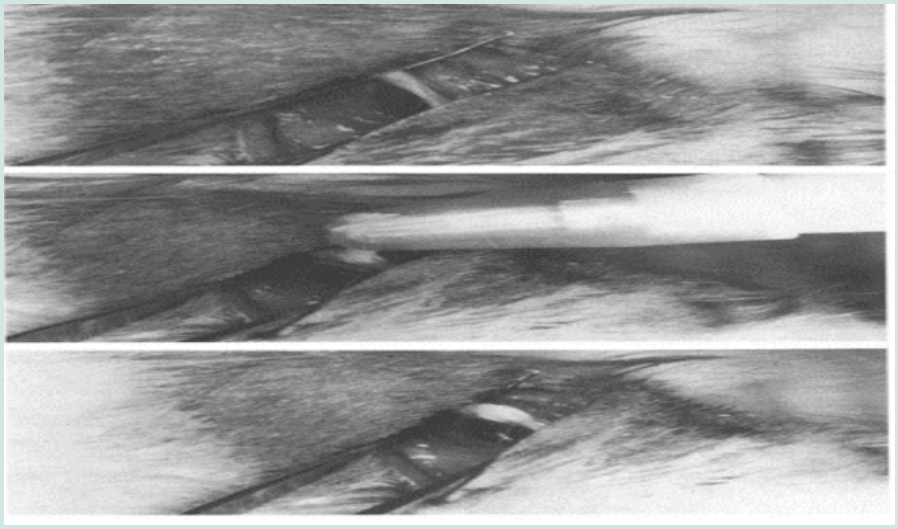

Figure 8: Surgical procedure of SCN using a modified clinical cryoprobe. The first panel demonstrates dissection of the common sciatic nerve proximal to its primary trifurcation. Instruments and surgical approaches are standardized to minimize nerve trauma. The second panel shows the cryoprobe placement on the sciatic nerve using a freeze-thaw-freeze cycle. The third panel shows the ice-hall formation immediately following the freeze [60].

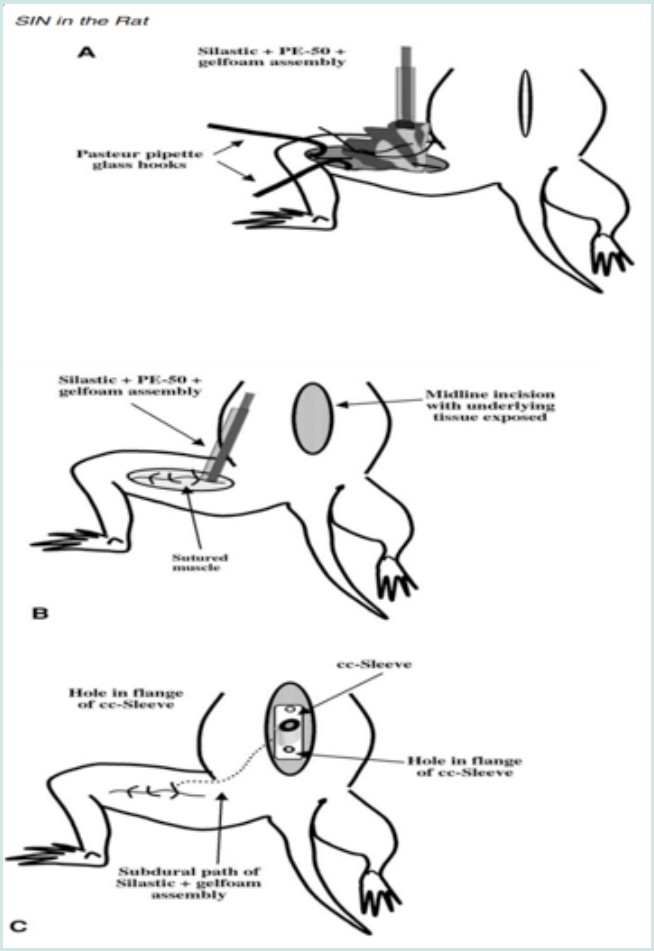

Figure 9: (A) The process of enwrapping the gelfoam portion of silastic + PE-50 + gelfoam assembly around the sciatic nerve, (B) Illustrating the exteriorized portion of the silastic + PE-50 catheter after the gelfoam has been implanted and muscle walls have been closed with sutures. (C) cc-Sleeve attachment to the lower back area after the silastic + PE-50 + gelfoam assembly has been implanted [74].

Figure 10: Posture change after laser irradiation. The typical posture includes mild elevation of the hind paw and flexion of the toes on the operated side particularly when walking on uneven surfaces [87].

Spinal nerve ligation (SNL)

An experimental animal model of peripheral mononeuropathy caused by SNL was created by Kim and Chung. Rats are sedated in this model, then their lower backs are shaved while they are lying on their backs. The left lumbar spinal nerves are then accessed by making a 2-cm-long incision at the level of the posterior iliac crest. Using 6-0 silk suture, the L5 and L6 spinal nerves are carefully identified, separated from the neighbouring L4 spinal nerve, and then firmly ligated distally to the dorsal root ganglia (DRG) [34,35]. Behaviour changes such mechanical allodynia, cold allodynia, thermal hyperalgesia, and spontaneous pain have been shown in this model to appear within 24–48 hours and last for 10–16 weeks [34,36,37]. It has been demonstrated that sympathectomy lessens the behavioural symptoms of neuropathic pain [38,39]; This paradigm is consequently known as an animal model of sympathetically mediated pain. The ligation location and extent are more constant in this model when compared to the CCI and PSL models [27,40]. By ligating the L5 spinal nerve, Labuda and Little created an L5 SNL model that is simple, highly repeatable, and causes less harm to the surrounding tissue and peripheral nerves than the L5/L6 SNL approach [37]. By tightly ligating the L7 spinal nerve, which is located just distal to the L7 dorsal root ganglion, Carlton used primates (Macaca fascicular is) to simulate the state of neuropathic pain. The monkeys displayed pain behaviours that were strikingly like those seen in people with peripheral neuropathic pain. When a significant and steady amplitude of pain behaviour is required, the SNL model has traditionally been the model of choice. The neuropathic pain sensations produced by the SNL model closely resemble those experienced by people with causalgia, which is caused by damage to the peripheral nerves [34,41].

Spared nerve injury (SNI)

Decosterd and Woolf created a brand-new animal model of neuropathic pain using this technique [44]. In this paradigm, rats are given general anaesthesia before having the skin on the left lateral thigh shaved and the biceps femoris muscle divided. The sural, common peroneal, and tibial nerves, together with the sciatic nerve, are all clearly visible. Then, 2 mm of the distal nerve is axotomized after the tibial and common peroneal nerves are firmly tied with 5-0 silk. The sural nerve is protected from injury by being avoided at all costs and is never touched or stretched. This model is known as the "Spared Nerve Injury (SNI) model" because only one nerve, the spinal, is spared while the other two nerves, the tibial and common peroneal, are amputated. The identical surgical procedures were used to create two variations of sciatic nerve SNI damage, but with distinct combinations of nerve transections. In one variant, the common peroneal and the sural nerves are sectioned, leaving the tibial nerve (t) intact (SNIv(t)); while in another variant, the tibial nerve is injured leaving the sural(s) and common peroneal (cp) nerves intact (SNIv(s,cp)) [45,46].

Within four days of the damage, mechanical and thermal hyperalgesia and allodynia have been seen, and they last for several weeks (up to six months) after the injury [44,45]. The ipsilateral sural and, to a lesser extent, the saphenous area exhibit greater reactivity to noxious and non-noxious stimuli [44,47]. It has been described that mice also show similar behavioural alterations, subjected to SNI as seen in rats [45,49]. This model differs from previous models of peripheral nerve damage, such as CCI, PSL, and SNL, in that it enables the evaluation of variations in the mechanical and temperature sensitivity of adjacent non-injured skin territory. This trait is crucial because it enables the simultaneous examination of alterations in both damaged main

sensory neurons and nearby uninjured sensory neurons, allowing for the exploration of their respective contributions to the pathophysiology of pain. Recent studies have emphasised the significant role that non-damaged neurons play in neuropathic pain, including abnormal sensory voltage-gated sodium channel expression, increased transient receptor potential channel (TRPV1), and activation of Schwann cells. Ectopic C-fiber activity is another example. The mechanical and thermal sensitivity alterations in this model are large, long-lasting, and closely resemble several aspects of real neuropathic pain [49]. In comparison to earlier versions, the surgical method for making this model is quite simple, and the degree of damage varies less often [44].

Tribal and sural nerve transection model

Lee et al. created a novel model of neuropathic pain called tibial and sural nerve transection. In order to expose the sciatic nerve and its three terminal branches, the sural, the common peroneal, and the tibial nerves, a section is made right through the biceps femoris muscle in this model while the patient is under anaesthesia. The sural and tibial nerves are then sectioned distally to the ligation to remove 2 mm of the distal nerve, and they are then securely ligated with 5-0 silk. The common peroneal nerve is protected by taking special precautions to prevent any touch, straining, or injury [50,51]. In this paradigm, mechanical allodynia, cold allodynia, chemical allodynia, mechanical hyperalgesia, and spontaneous pain have all been described as significant and dependable neuropathic pain sensations [50,52]. Most of these behavioural alterations begin on the third day following surgery, peak in 1-2 weeks, and last for 1-12 months. However, in this neuropathic pain paradigm, heat allodynia has not been proven [20]. According to Han et al., neuropathic pain in this model is SIP [50]. Additionally, this kind of model may be created rather easily. Because of this, this animal model is extremely helpful for understanding the mechanics of neuropathic pain, particularly SIP, and testing medications for its treatment [52].

Ligation of the common peroneal nerve

The evaluation of the sensory system is made more challenging in most animal models of neuropathic pain because both sensory and motor nerves are damaged, resulting in aberrant sensory and motor responses. Therefore, model behavioural nociceptive responses should be elicited in animals under a neuropathic pain scenario that does not compromise motor function or cause muscle damage (Figures 11-15). By ligating the common peroneal nerve using chromic gut suture 5-0 without disrupting the blood vessels, a new mouse model of neuropathic pain has been created. The nerve is wrapped in a single knot, which is then gradually tightened. The endpoint of the ligature's tightening is determined at the point at which the dorsiflexors of the foot begin to twitch and are visible at the digits. With intact motor functions, long-lasting behavioural allodynia and thermal hyperalgesia have been seen [54].

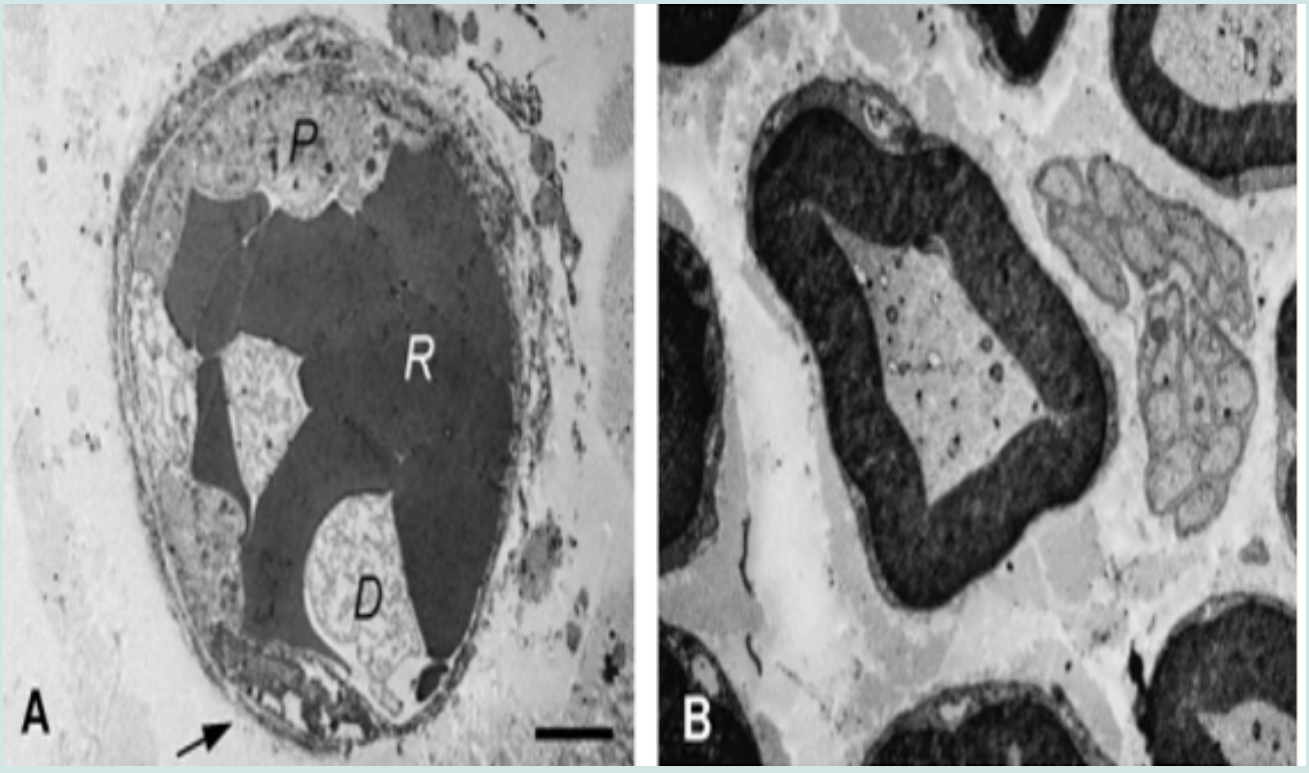

Figure 11: Electron micrographs in the irradiated segment of the sciatic nerve 5 min after laser irradiation. (A) The formation of thrombi was noted in epineurial vessels 5 min after laser irradiation. Endothelial cells of the epineurial vessel were severely damaged with formation of vacuoles (arrow). The components of the thrombi included red blood cells (R) and granulated (P) and degranulated (D) platelets. (B) Immediately after laser irradiation, myelinated and unmyelinated axons appear normal in the central region of the nerve fascicle. (Bar, 2 Am in A and B) [87].

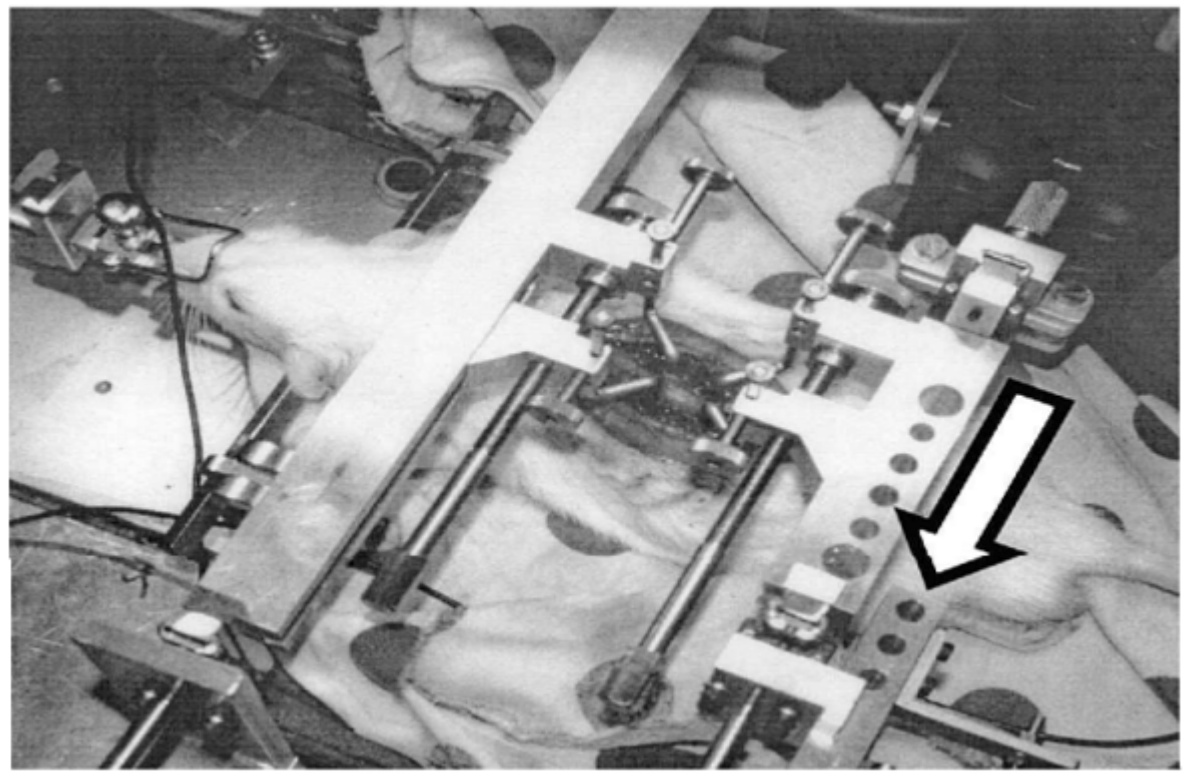

Figure 12: Schematic of device. The animal's head and upper spine are immobilized by the stereotaxic frame and clamps fixed to the top beam. The lower spine is fixed to the lower beam, which is translated to the left to create the injury [98].

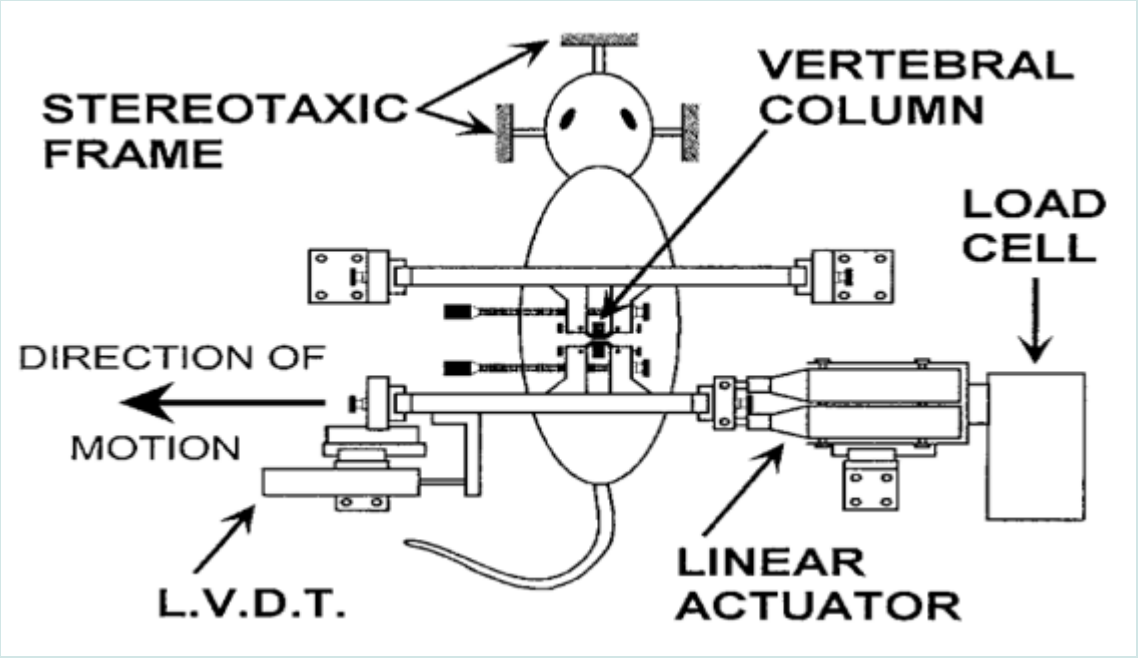

Figure 13: Photograph of rat in device. The beam on the right-hand side undergoes the translation in the direction indicated by the arrow [98].

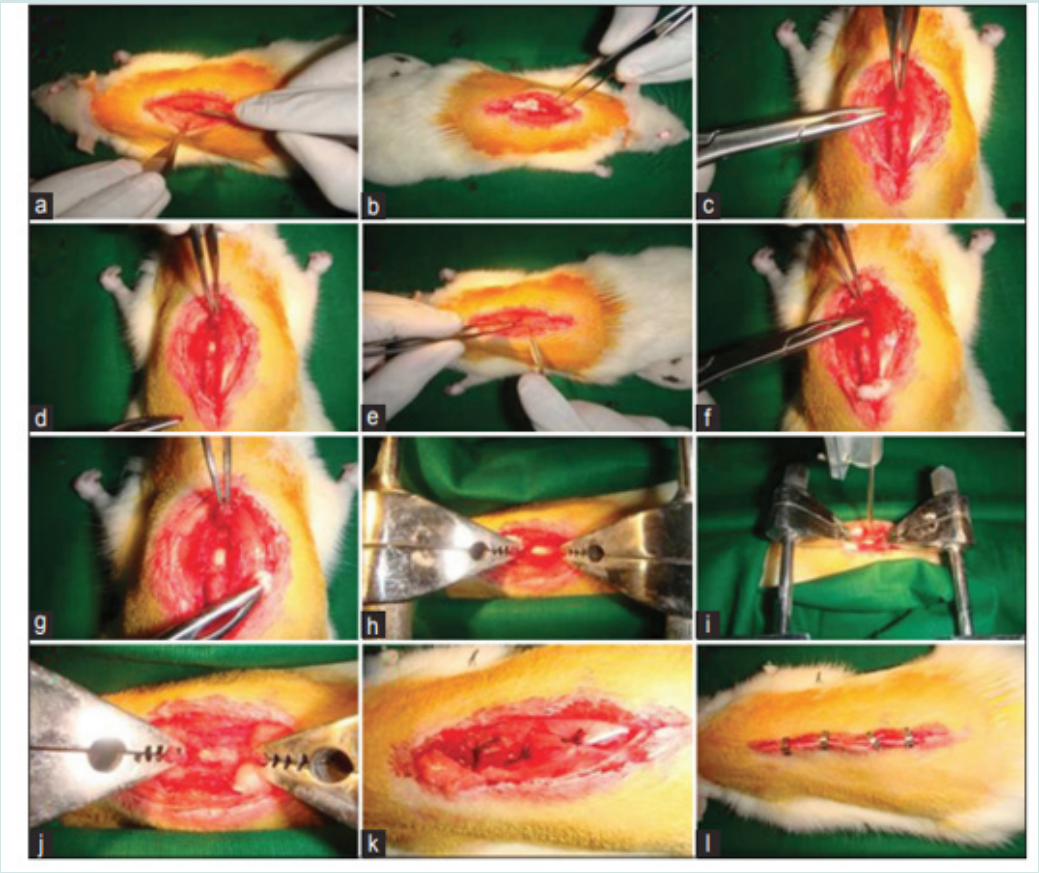

Figure 14: Laminectomy and contusive spinal cord injury at T10 T12 level (under Ketamine [80 mg/Kg] and xylazine [10 mg/kg]). Contusion created using customized impact device for aneathetized control and experimental animals which were grouped as per study design. Surgery was performed under highly sterilized condition with extreme post operative care. (a e) Vertebrae exposed; (f h) Laminectomy; (i j) Injury created with clamp; (k l) Injury site was sutured and closed [99].

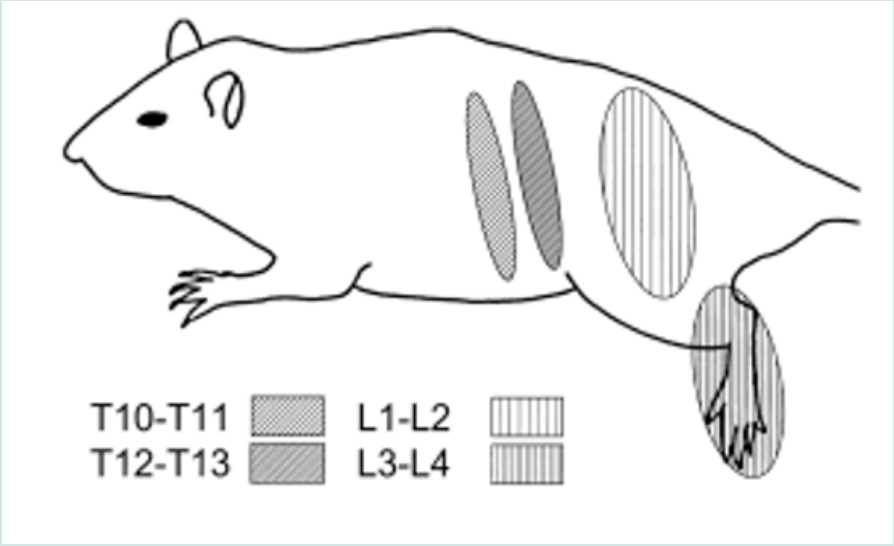

Figure 15: Topographic distribution of areas targeted for excessive grooming behaviour as a function of spinal segments injected with quisqualic acid (QUIS). Excessive grooming behaviour was directed towards skin areas in dermatomes of spinal segments at or caudal to those receiving QUIS injections. The areas outlined on the line drawing summarize the location of all areas affected by excessive grooming behaviour (Classes I-IV) following injections in segments shown in the inset. As injection sites moved from rostral (T10–T11) to caudal (L3–L4), the location of sites targeted for excessive grooming behaviour moved down the body from thoracic to hind limb dermatomes [107].

Sciatic cryoneurolysis

The fact that no transection or ligation is performed makes this type of an intriguing animal model of peripheral neuropathy. Instead of this, sciatic nerve freezing has been utilised to cause nerve damage. In this illustration, the sciatic nerve is gently dissected from the surrounding tissue and raised with forceps after a dorsolateral incision is made at the level of the thigh. The nerve is then chilled to 60 C using nitrous oxide as a refrigerant, frozen with a cryoprobe [58,59]. Proximally to its trifurcation. In a 30/5/30 s freeze/thaw/freeze cycle, the sciatic nerve is probed with a 2-mm cryoprobe tip. The cut is stitched together, and the nerve is placed back in place after recovering for 20 seconds. This type causes mechanical allodynia and autotomy but not thermal hyperalgesia as symptoms. In the first seven days following injury, the cry neurolysis model reveals no variation in pain behaviours [59]. In contrast to the significantly longer persistence of pain behaviours in SNL, PSL, and SNI, behavioural indicators generated by this model only last for 15–21 days [58].

Caudal trunk resection

The S3 and S4 spinal nerves are separated from the left inferior caudal trunk of the rat in this model. Mechanical, thermal, and heated allodynia can develop in the tail and remain for a few weeks. Mechanical and thermal allodynia symptoms can be seen the day following a nerve damage [61]. In a comparable sort of animal, the S1–S3 spinal nerve innervations to the tail are removed by exposing and cutting the left superior caudal trunk between the S3 and S4 spinal nerves [62]. Alternately, animals can have the S1 spinal nerve, which innervates the tail, removed by unilateral transection of the inferior and superior caudal nerve trunks between the S1 and S2 spinal nerves. Pieces of the nerve (approximately 2 mm in length) are excised from the distal nerve ends to avoid the potential of re-joining of the proximal and distal ends of the severed trunks [63]. Within a day of the damage, mechanical allodynia and cold/thermal hyperalgesia begin to manifest and remain for several weeks. Additionally, mouse models that include cutting the left inferior and superior caudal trunks of the S1 spinal nerve have been produced [64]. Another model imitates the damage approach reported by Sung et al. by exposing and transecting the left superior caudal trunk between the S3 and S4 spinal neurons [62]. The S1–S3 spinal nerve, which innervates the tail through the superior caudal trunk, is removed during surgery [65].

Sciatic inflammatory neuritis (SIN)

According to estimates, inflammation, or infection rather than trauma account for close to half of all neuropathies in humans [66]. Furthermore, inflammatory processes continue to develop even after acute nerve damage. As a result, a neuritis model has been created and is the preferred model for many research teams to cause nerve injury. The catheter is surgically implanted around the sciatic nerve while the rats are under anaesthesia. The peri-sciatic catheters are made of sterile gel foam and aseptically cut into strips, with one end being split in half to enable silastic tube suturing from the inside (Figures 16-20). Gel foam is threaded around the left sciatic nerve after it has been exposed at mid-thigh level by blunt dissection, and the external end of the catheter is then inserted subcutaneously to the midline, just rostral to the tail base. 4-5 days following surgery, the catheter is utilised for a single injection, which is administered to freely moving rats by putting PE-50 tubing via the silastic catheter. To eliciting SIN, a single focused injection of zymosan (yeast cell walls) in dosages ranging from 4 mg (low dose) to 40–400 mg (high dose) is made around the sciatic nerve [67,68]. The pro-inflammatory gut suture and pro-inflammatory cytokine production stimulator high mobility group protein (HMG) and tumour necrosis factor (TNF)-alpha injections have also been used to activate the peri-sciatic immune system and cause dose-dependent unilateral and bilateral hind-paw mechanical allodynia [69,70].

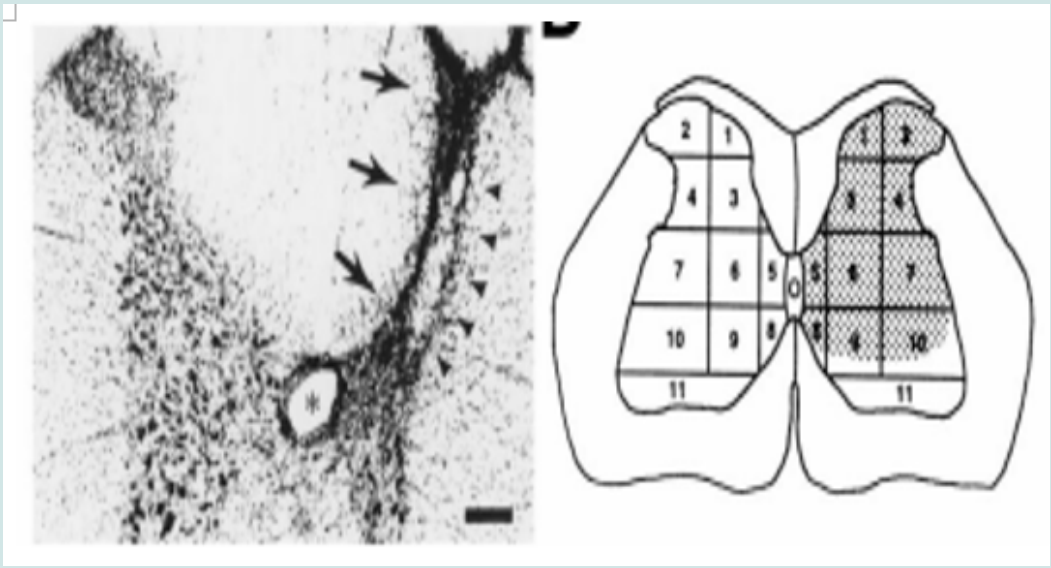

Figure 16: Photomicrograph showing the pattern of neuronal loss including spinal regions 1–10 (arrows). Note dilated central canal (*) and the slender cavity in the dorsal horn (arrowheads). Scale bar, 190 mm, Schematic representation on a standard cross-sectional drawing of the spinal cord showing the pattern of neuronal loss in first one [107].

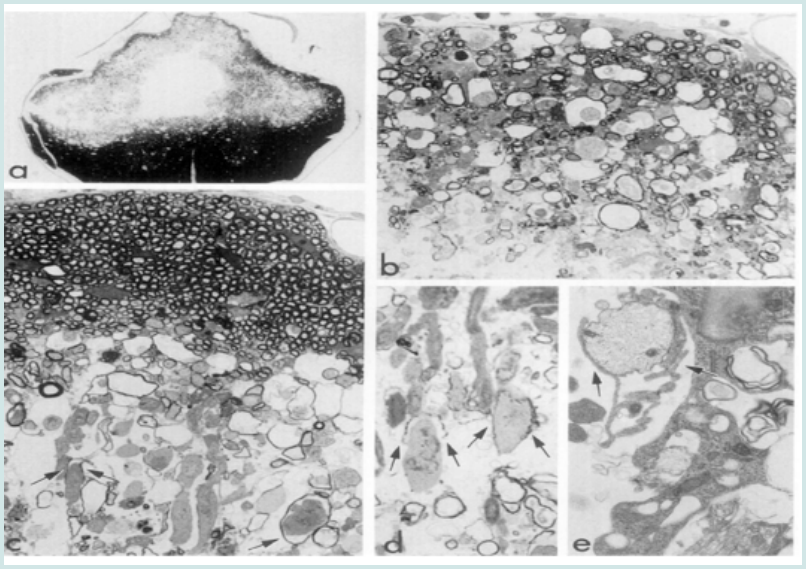

Figure 17: 2 and 5 dpl. At the lesion epicenter the necrotic area extended across most of the spinal cord diameter and from the dorsal surface to a level near the central canal (a). The degeneration extended to the meninges dorsomedially (b) but, more laterally, the spinal cord rim was spared (b, far right; c, lateral spinal cord, the edge of which is at the top of the panel). In the area of degeneration, swollen axons (either longitudinally or cross-sectioned) were apparent, and portions of them were surrounded by myelin debris (arrows) (c, d). Some axons may have been stripped of myelin (demyelinated) because phagocytic processes (arrows) we seen in electron micrographs (e) to have surrounded them. The axon in e is adjacent to a debris-laden macrophage. (a, e) 5 dpl; (b-d) 650*; (c) 600* ; (e) 16,000* [112].

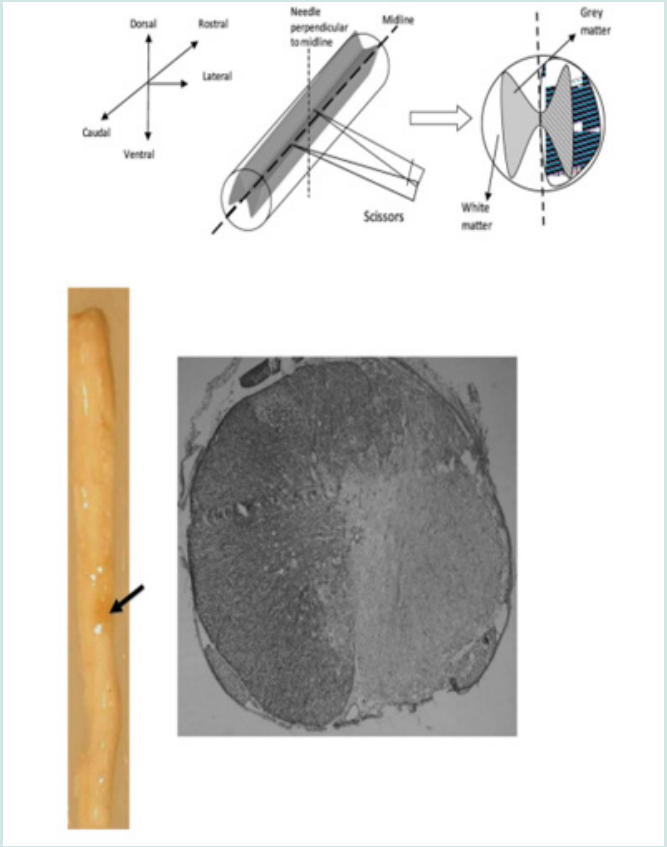

Figure 18: A schematic of the hemisection surgery. Also shown is a transverse cross section of the hemisected spinal cord. The light micrograph shows an injured spinal cord. The arrow points toward the injured portion. A representative cross section of the injury site is also shown [115].

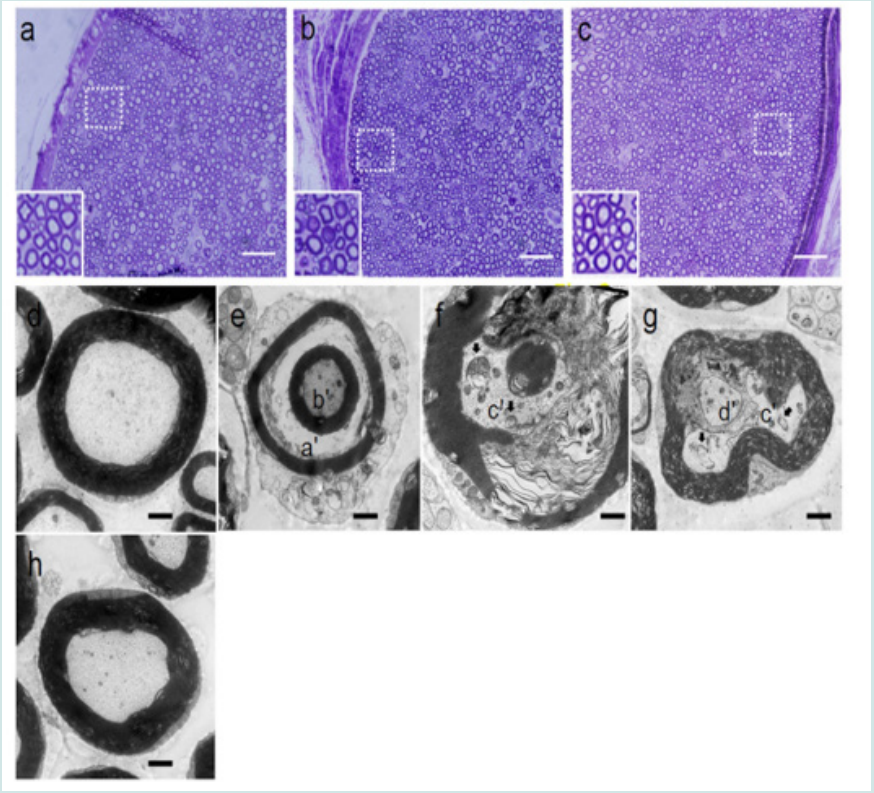

Figure 19: Oxaliplatin (L-OHP)-induced axonal degeneration in rat sciatic nerve and goshajinkigan (GJG)-ameliorated axonal degeneration of the sciatic nerve. Histological analysis of the sciatic nerve was performed at 8 wks. (a–c) Representative cross sections of the sciatic nerve by light microscopy. The sciatic nerves were isolated in vehicle-treated (a), L-OHP+ DW-treated (b) and L-OHP+ GJG (1 g/kg)-treated rat (c), and then stained with toluidine blue. Scale bar= 100μm. (d–h) Representative pictures of the sciatic nerve by electron microscopy. (d) Axons of myelinated fiber in vehicle-treated rat. (e) Myelin sheath (a′) by atrophy of axon (b′) in L-OHP+ DW-treated rat. (f) Accumulation of organelles (c′), vacuolated and swollen mitochondria (arrows) in degenerative axon of L-OHP+ DW-treated rat. (g) Infiltration of macrophage (d′) in myelin sheath and phagocytosis of degenerative axon in L-OHP+ DW-treated rat. (h) A representative cross section of axon treated with GJG. Scale bar= 10μm [151].

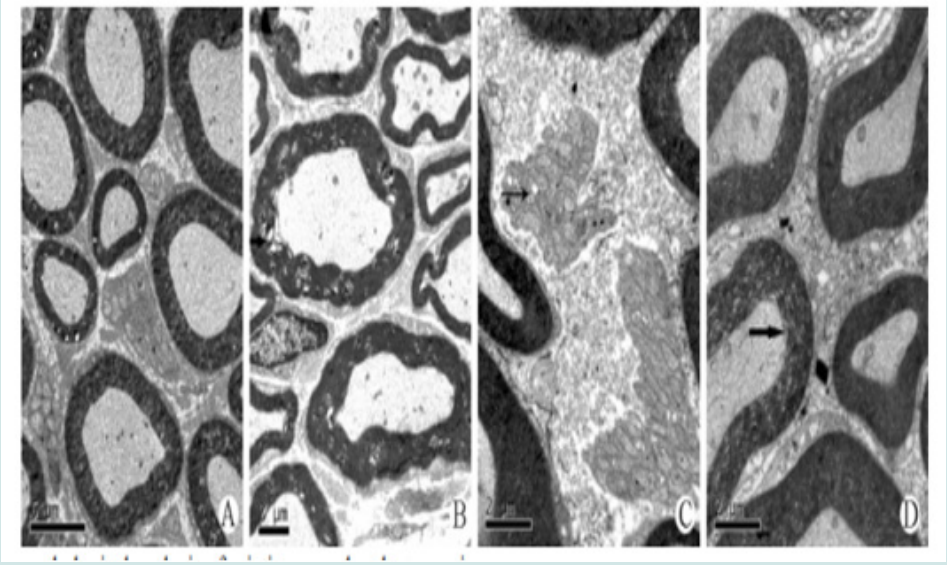

Figure 20: 3 Neuropathological analysis of sciatic nerves by electron microscope (A) Naive control, group 1; (B), (C) Docetaxel treated group, group 2; (D) Pregabalin 30 mg/kg treated group, group 5 (n=2). More severe impairment of nerve fiber is observed in group 2 as compared to group 5. The black arrows in (B) and (D) show demyelination in myelinated fiber. The black arrow in (C) shows vacuolation in unmyelinated fiber [164].

Also found to elicit an immunological response and cause mechanical allodynia is the injection of dead bacteria (the active ingredient in complete Freund's adjuvant) or carrageenan (seaweed protein) to the sciatic nerve. These increases in discomfort were often noticeable the next day and peaked two to three days following surgery [71]. A perplexing phenomenon linked to damage or inflammation to the peripheral nerves, mirror-image pain originates from areas contralateral to the site of injury. Atypical face pain, causalgia, reflex sympathetic dystrophy, idiopathic facial erythromelalgia, and steatopygia are a few chronic pain syndromes that cause mirror-image discomfort [72,73]. Mechanical allodynia, or discomfort felt in reaction to gentle touch or pressure stimuli like clothes and bed linens, is a common characteristic. The creation of the sciatic inflammatory neuropathy (SIN) model has lately made it easier to examine mirror image neuropathic pain [67,68]. A unilateral mechanical allodynia develops ipsilateral to the inflamed sciatic nerve due to the low degree of immune activation. However, higher immune activation results in bilateral allodynia that affects the ipsilateral and contralateral sides of the inflammatory nerve condition [67,68].

Cuffing of sciatic nerve-induced pain

In this model, rats' common branches of the sciatic nerve are surgically implanted with a polyethylene cuff measuring 2 mm in length and 0.7 mm in inner diameter [75,76,77]. This concept has recently been reported in mice as well [78]. Heat-hyperalgesia, which lasts for three weeks, and mechanical allodynia, which lasts for two months, are characteristics of the neuropathic pain model [79]. Fixed-diameter polyethylene cuff application has been shown to cause nicafenine reactions in rats as well as changes in the fibre size spectrum in the peripheral nerves. Inflammatory responses and concurrent anterograde Wallerian degeneration are also present. There is also a brief drop in the number of unmyelinated and tiny myelinated axons. It has also been shown that the constellation of behavioural and morphological abnormalities brought on by cuff neuropathy are comparable to those brought on by Bennett and Xie's CCI model, with the significant benefit of a more uniform degree of nerve damage in terms of fibre spectrum modifications [15, 75]. In this model, standardised cuff implantation affords a high degree of consistency around the sciatic nerve. The cuffing-induced neuropathy model has been employed by several research teams to investigate the molecular causes of central sensitization [77,80] and the ways in which antidepressant medications work to treat neuropathic allodynia [78,81].

Photochemical-induced sciatic nerve injury.

In this model, the left sciatic nerve is surgically exposed to an argon ion laser with an average power of 0.17 W operating at a wavelength of 514 nm for 30 s to 2 min after receiving an intravenous injection of the photosensitizing dye erythrosine B (32.5 mg/kg) through the tail vein. To separate the nerve from the surrounding tissue and reflect light, aluminium foil is positioned beneath the nerve [82,83]. It has been established that the photochemical reaction that forms thrombosis and occlusion in the tiny capillaries supplying the nerve, rather than the heat produced by the laser, is what causes nerve damage. This model has been shown to exhibit highly repeatable mechanical, heat, and cold allodynia, as well as symptoms of spontaneous pain [83]. By lasering the sciatic nerve after injecting a photosensitizing dye into it, a mouse model that exhibits demyelination and axonal degeneration has also been created [84].

Laser-induced sciatic nerve injury

The concurrent necessity of photosensitive dyes is one possible drawback of the prior concept. However, investigations using laser irradiation have shown that using a CO2 laser alone might cause variable degrees of Wallerian degeneration [85]. In this model, a diode-pumped solid-state laser operating at 532 nm with an output power of 100 mW is used to irradiate the epineurial vasculature of the sciatic nerve for 30 seconds after marking the portion of the sciatic nerve immediately distal to the gluteus muscle with epineurial sutures. There is a significant decrease in the blood flow to the nerve after laser irradiation [86]. Animals begin to exhibit typical neuropathic pain symptoms on the second post-operative day, such as mechanical allodynia, thermal hyperalgesia, and spontaneous pain behaviours. After surgery, these phenomena reach their height and persist for 3-6 weeks [2].

Central pain models

Several central pain models have been created based on the SCI. Dysesthesia and pain, including spontaneous and evoked, are characteristics of SCI caused by trauma, ischemia, compression, or crushing [88-92].

Weight drop or contusive SCI (Allen's Model)

The weight drops or contusion model is the most traditional and often applied SCI model. The lower thoracic-lumbar spinal cord is exposed in this model, and a steady weight is put over the nerve to cause an injury that results in severe paraplegia and total segmental necrosis [88]. Various researchers have modified this model to consistently regulate the severity of the damage. Laminectomy is done in the vertebral lower thoracic-lumbar region (T-10) level after anaesthesia to expose the dorsal spinal cord. The exposed cord is supported by a brass guide tube that is 15 cm long and perpendicular to it (Figures 20-26). A cylindrical 10 g steel weight with a rounded tip is hung within the tube. To cause cord damage, the weight is permitted to fall onto the exposed chord at the segmental level of T12–13. One day after an injury, it has been shown that the skin becomes hypersensitive to mild mechanical stimulation. This development is like how quickly people acquire allodynia after suffering a spinal injury [88,93-96]. As an alternative, the paravertebral muscles are divided, and a longitudinal incision is created in the midline of the back to expose the T8 vertebrae. To expose the spinal cord, it is followed by a four-level T6–T7 laminectomy. Injury is then caused by extradural compression of the spinal cord using a 24 g aneurysm clip [97].

Excitotoxic spinal cord injury

a-amino-3-hydroxy-5-methyl-4-isoxazolepropionic acid (AMPA) metabotropic receptor agonist Quisqualis acid (QUIS) injections into the spinal fluid have been used to mimic injury-induced increases of excitatory amino acids, a well-known neurochemical complication of spinal cord injury [98-100]. The increasing pathological alterations brought on by QUIS injections mimic those documented after ischemia and traumatic SCI quite a bit [100,101]. They strikingly re-

semble post-traumatic syringomyelia, a clinical disorder [102,103]. At levels ranging from T10 to L4, the unilateral injections are administered between the dorsal vein and the dorsal root entrance zone at depths ranging from 300 to 1200 mm below the spinal cord's surface [104,105]. The intraspinal injection of QUIS is designed to cause excitotoxic damage, which results in neuronal death in certain areas of the spinal grey matter, and to elicit "spontaneous" and/or "evoked" pain responses that are comparable to those described in other models of SCI [89,90,95] and neuropathic pain [15]. Thus, it has been established that the excitotoxic model is a useful tool for investigating the primary mechanism(s) and neural substrate(s) in charge of the onset and development of altered sensory experiences after SCI. infusions of glutamate, N-methyl-D-aspartic acid, or kainic acid intravenously or intrathecally [2-5,6-15]. des-Tyr-dynorphin Serotonin, tryptamine, and peptides have all been linked to pain-related SCI behaviours [106].

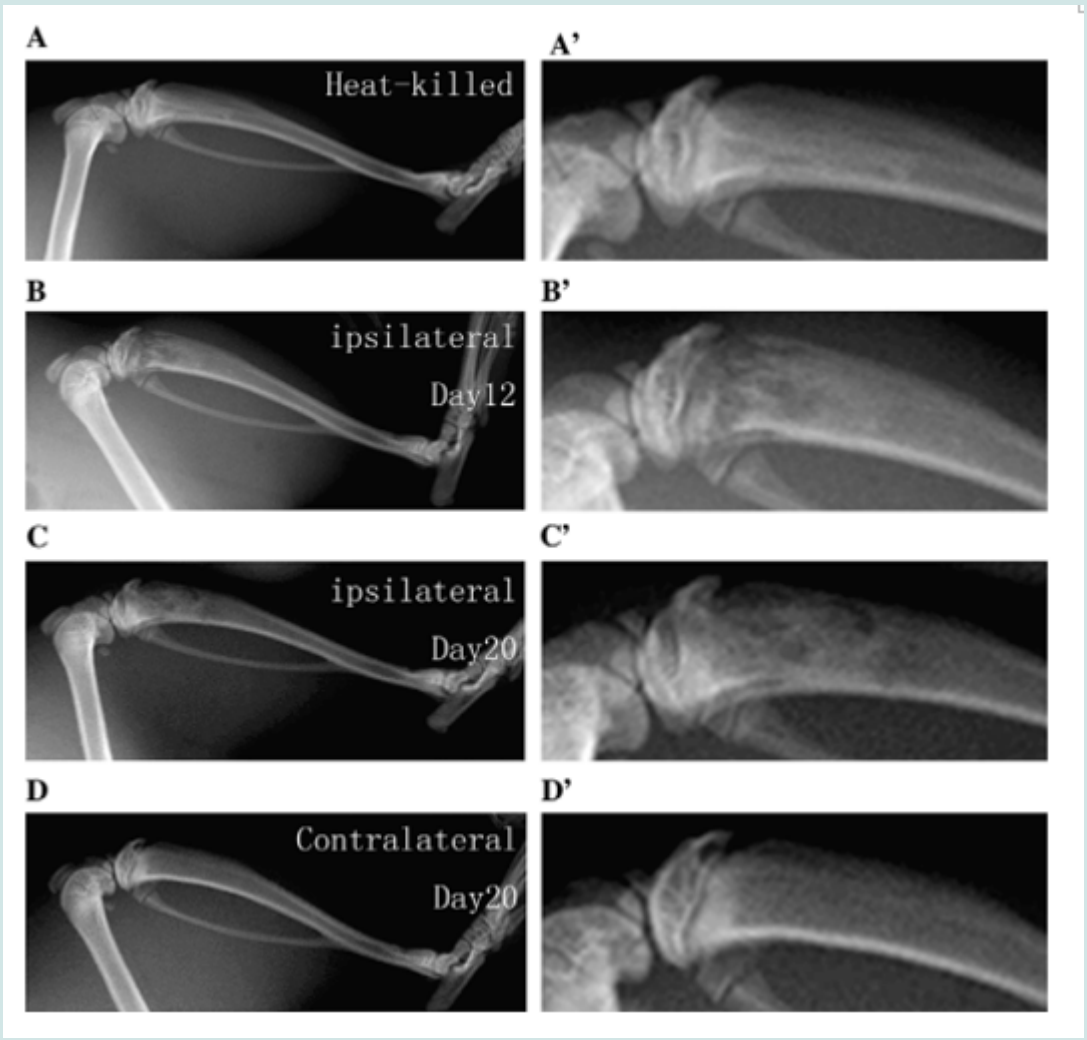

Figure 21: Radiographs of the tibia bone inoculated with heat-killed Walker 256 cells (A), and live Walker 256 cells 12 and 20 days after inoculation in the ipsilateral (B and C) and contralateral (D) hind limbs. (A0 –D0) showing the proximal end of the bones with a higher magnification. Radiograph of the ipsilateral Walker 256 injected and the contralateral tibia from the same animal, 20 days after inoculation. Note the lack of any effect on the contralateral side [206].

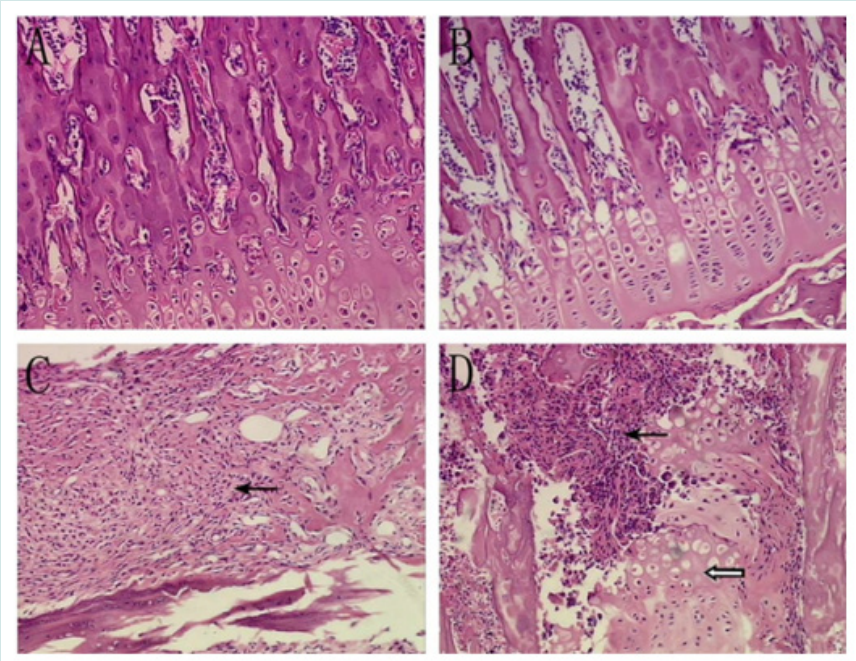

Figure 22: Histology of tibial bone destruction (Hematoxylin-eosin stain). The sections (7 lm) were taken from tibial bone 20 days after surgery. (A) Bone injected with PBS; (B) bone injected with heat-killed cells; (C) showing tumor growth and bone destruction after injected with 4 ·105 Walker 256 mammary gland carcinoma cells (tumor cells are marked by black arrow); (D) showing newly formed bone after injected with 4 ·105 Walker 256 mammary gland carcinoma cells (tumor cells are marked by black arrow while newly formed bone is marked by hollow arrow) [206].

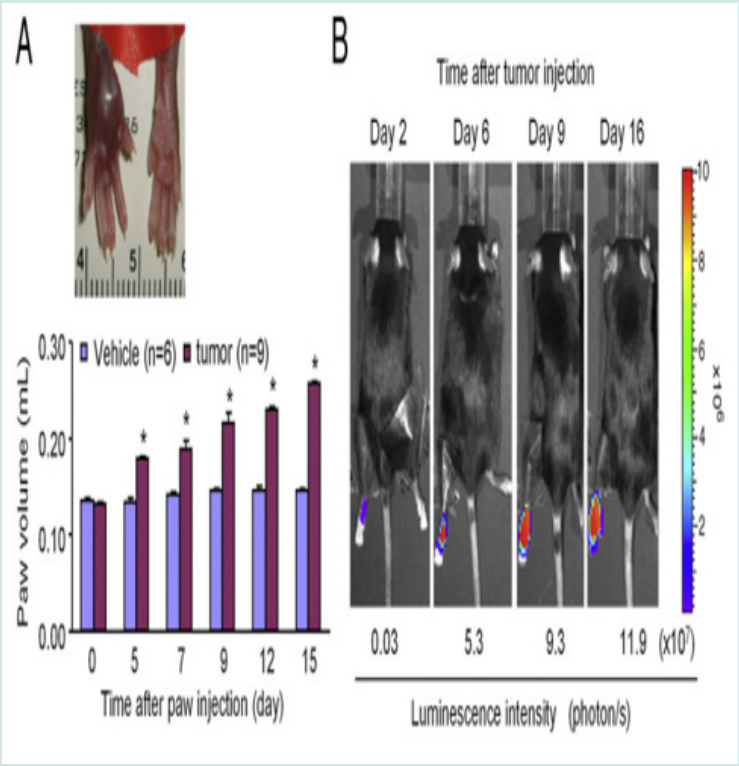

Figure 23: Time course of tumor growth and cancer pain development following intraplantar injection of luciferase-transfected B16-Fluc melanoma cells. (A) Increase of paw volume after inoculation. Inset shows the tumor-bearing hindpaw (left) 15 days after inoculation. (B) Bioluminescent imaging shows enhanced luminescence intensity over time in an inoculated hindpaw, indicating a continuous growth of melanoma [219].

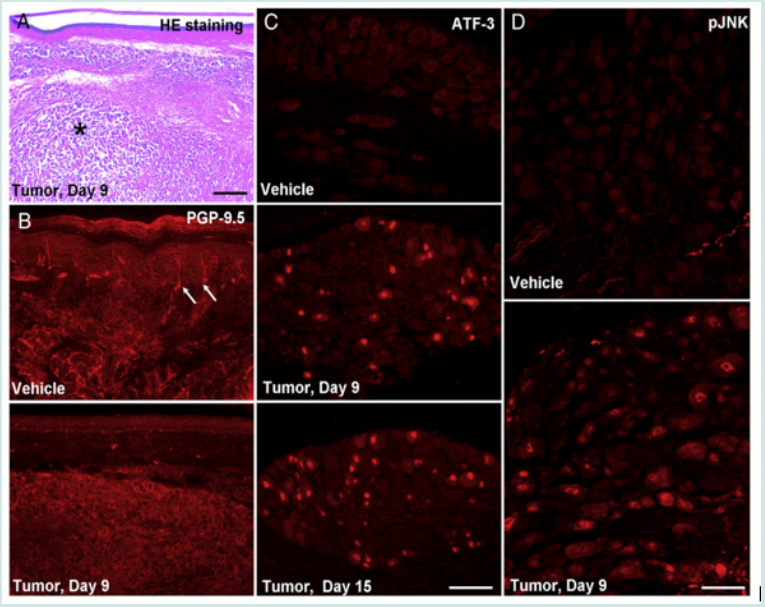

Figure 24: Nerve degeneration in the tumor-bearing hindpaws. (A) Hematoxylin–eosin (HE) staining of hindpaw skin (plantar surface) 9 days after tumor inoculation. The tumor tissue (indicated with *) was located in the dermis. Scale bar, 400 μm. (B) PGP-9.5 immunostaining of hindpaw skin (plantar surface) reveals a loss of nerve fibers 9 days after tumor inoculation. Arrows indicated nerve fibers in the epidermis. (C) ATF-3 immunostaining indicates induction of ATF-3 in the nuclei of many DRG neurons after tumor inoculation. Scale bar, 100 μm. (D) pJNK immunostaining shows JNK activation in DRG neurons after tumor inoculation. Scale bar, 50 μm [219].

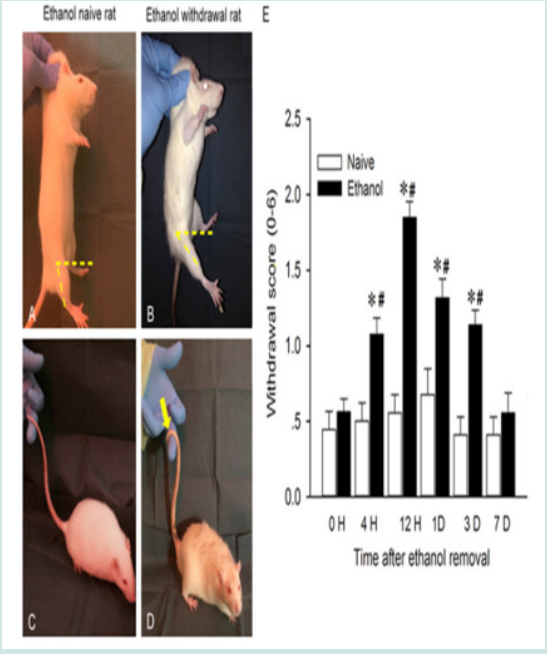

Figure 25: Physical dependence syndromes in SD rats withdrawn from chronic ethanol administration. After consuming ethanol intermittently for 12 weeks, the physical withdrawal syndrome was observed and quantified (on a scale of 0-2) during one week of alcohol removal. The left panels are representative photographs showing the increased score derived predominantly from positive signs of lower limb flexion and tail stiffness 12 h after alcohol removal, when comparing to ethanol naïve SD rats. Note that the smaller angle between horizontal axis and longitudinal axis of lower limb indicates an obvious flexion of the hip joint in withdrawn rats (B) compared to alcohol-naïve rats (A). An observation of the rat tail tip wrapped around the observer's finger (yellow arrow in D) was found in withdrawn rats but not in alcohol-naïve rats (C). The right panel shows the withdrawal scores, determined by summing the scores for all three symptoms, significantly increased at 4 hr, peaked at 12 hr and lasted for 3 days, compared to alcohol naïve rats. (All $P < 0.001$, $n = 25$) [242].

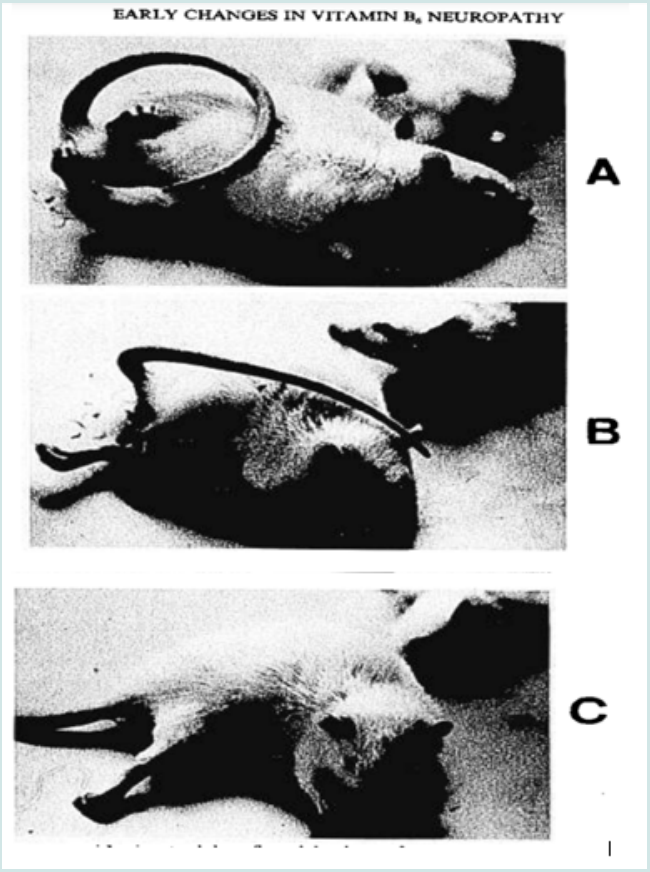

Figure 26: Severe pyridoxine toxicity after eight days treatment. A rat, deliberately placed on its back (A), corrects its position by a vigorous swing of the tail and padding movements of the hind legs (B); it is unable to walk (C) [251].

Photochemical SCI

In this model, erythrosine B, a photosensitizing dye, is intravenously administered after which the vertebrae are surgically exposed to an argon ion laser, which causes excitation and leads to regional blood artery blockage [107]. It has been established that the nerve damage is not caused by the laser's heat, but rather by a photochemical reaction that causes thrombosis in the tiny blood capillaries that nourish the nerve. It has been demonstrated that after photochemical irradiation, local blood flow in the spinal cord is significantly decreased. At the level of the spinal cord, this spinal ischemia event is linked to parenchymal tissue necrosis [89,108,109]. These neuropathic pain characteristics, including autotomy, mechanical and cold allodynia, and hyperalgesia, have been seen in this model [89,110,111].

Spinal Hemisection

This model has been used extensively as a central pain model because it has a variety of benefits, including regular control over the quantity and kind of damaged fibres in each animal. Second, the damaged and unharmed sides are entirely divided. Laminectomy is done at the T11-T12 segments after a longitudinal incision is created to expose the various spinal cord segments. A blade is used to hemissect the spinal cord just cranial to the L1 dorsal root entrance zone, which causes mechanical and thermal allodynia to occur [90]. This neuropathic pain model substantially develops mechanical and cold allodynia in the tail as well as the limbs. Additionally, allodynia persists for a very long period after spinal cord hemisection [112,113]. Brown-Sequard Syndrome (BSS), a prolonged state of excruciating agony, is observed on both sides below the lesion in human spinal cord hemisection injuries. Ipsilateral hemiplegia and contralateral hyperalgesia are features of the BSS [11]

Drug-induced neuropathy models

Anti-cancer agents-induced neuropathy models

In most individuals with this dosedependent neuropathy, painful paresthesias are the initial symptom. More so than the vibration sense are the pinprick and temperature sensations. The loss of axons and motor capabilities become more noticeable in the latter stages of the illness [116], exerts significant effects on the peripheral nervous system, resulting in endoneurial edoema and microtubule disarray in both myelinated and unmyelinated sensory axons [117,118] C fibre nociceptive neurons' hyperresponsive activity is also seen [119]. To examine the pathogenic pathways involved in the emergence of neurotoxicity as well as the electrophysiological and histological alterations brought on by chemotherapeutic drugs, many animal models of vincristine-induced neuropathy have been created. Gottschalk et al. [120]. Later on, it was shown that receiving vincristine in numerous

dosages (20, 75, 100, or 200 lg/kg i.v.) via tail vein injection, followed by 500 l of saline to avoid artery degradation (days 1–5, then 8–13, Monday through Friday for 2 weeks), caused a painful neuropathy with a sudden start [117,119,121]. Because most rats exhibit relatively little motor impairment and maximum hyperalgesia, the 75 lg/kg i.v. dose regimen has been chosen. Switzer and others Sweitzer et al. [122], a study that used vincristine (75 lg/kg, i.v., on days 1–5 and 8–11 with nine doses) to treat neuropathy. According to reports, mechanical allodynia begins to appear on the fourth day following vincristine administration, peaks on the eleventh day, and starts to subside on the fifteenth. However, at cumulative doses >1000 lg/kg, motor performance and moderate to severe impacts on overall health are seen. Furthermore, considerable mortality from vincristine at high doses has also been documented [121,122]. Later, Authier et al., updated the model once more with a new medication dosage schedule. There have been no reports of a substantial impact on general health following the administration of vincristine to rats on an alternate-day schedule (total five administrations at dosages of 50, 100, 150 lg/kg i.v. with cumulative doses of 250, 500, 750 lg/kg, respectively). But vincristine at 150 lg/kg is known to cause behavioural alterations like mechanical and thermal hyperalgesia and allodynia, electrophysiological alterations like a decrease in sensory nerve conduction velocity (SNCV), and histopathological alterations characterised by the degeneration of axonal parts of myelinated nerve fibres. Because considerable nociceptive signals arise while maintaining good overall health and motor function, this paradigm has been shown to induce stable neuropathy [123]. Another animal model that uses a single dosage of vincristine (50, 100, or 200 lg/kg intravenously) to induce neuropathy has been described. After 5 days of vincristine treatment, mechanical allodynia and mechanical hyperalgesia emerge [124,125]. In order to distribute vincristine sulphate (30 mg/kg/day), rats have been surgically implanted with mini-osmotic pumps in the right external jugular vein as part of an animal model of neuropathy [126]. After a week following vincristine infusion, there has been an association between the development of severe mechanical and cold allodynia, with no impact on mechanical or thermal nociception. A novel model has recently been introduced in which vincristine (50 lg/kg i.p.) is given for 10 straight days while being monitored for 42 days [16,127,128]. Neuropathic pain has also been demonstrated to be induced by the administration of vincristine at a constant dose of 0.2 mg/kg or an escalating dose of 0.1 mg/kg by an increment of 0.05 mg/kg/week, given once weekly for five consecutive weeks with a total cumulative dose of 1 mg/kg. According to the clinical, electrophysiological, and histological data, vincristine causes axonal-type peripheral sensorimotor neuropathy, which is more pronounced in the fixed-dose group than the increasing-dose group [129]. Norido et al. used rabbits as an animal model for vincristine-induced peripheral neuropathy [130]. Vincristine has been shown to cause neurotoxicity, axonal swelling, and peripheral nerve regrowth in rabbits [131]. It is common practise to examine the effectiveness of neurotrophic factor and analgesic medications in neuropathic pain with a total of five consecutive doses of vincristine which is described by Authier et al. [123]. However, Siau and Bennett model is more useful for analysing electrophysiological research and histological alterations connected to chemotherapy drugs [127].

Platinum compound-induced neuropathy models. Cisplastin-induced neuropathy:

Cisplatin has demonstrated its efficacy in treating several cancers, including ovarian, testicular, colon, head, and neck, as well as lung cancer [132]. The use of platinum-derived antineoplastic medicines has been linked to emesis, anorexia, myelo-suppression, ototoxicity, nephrotoxicity, and peripheral neuropathy [133]. Both big and small diameter sensory fibres are affected by the peripheral sensory axonal neuropathy caused by cisplatin. After a cumulative dosage of 300 mg/m2, it typically produces clinical signs and symptoms in the classic "glove and stocking" way, and neuropathy may last for years [134,135]. Cisplatin-induced neurotoxicity in rats was investigated by Koning et al. However, because nephrotoxicity first appeared before neurotoxicity, it has been extremely challenging to create a cisplatin-induced animal model of peripheral neuropathy. Furthermore, it has been challenging to determine if neuropathy is a direct result of cisplatin or is a side effect of renal failure [136]. By paying close attention to water and dosage regimen, this challenge has been lessened. It has been demonstrated that neuropathy can develop after receiving cisplatin doses of 1 and 2 mg/kg once weekly for 9 weeks. Preclinical research frequently employs this neuropathy model [137,138]. Another model has been created that calls for administering cisplatin intravenously twice per week over a period of four weeks at a dosage of 2 mg/kg [139]. Another model of cisplatin-induced neuropathy has been created, involving the use of a different cisplatin dosing schedule, such as 1 mg/kg three times weekly or 2/3 mg/kg twice/once per week for five weeks [140]. The development of mechanical and cold allodynia, as well as thermal hyperalgesia, have been linked to cumulative dosages (15 mg/kg) [133]. Large, myelinated nerve fibres have shown axonal degeneration at dosage levels of 2 and 3 mg/kg, although unmyelinated axons show no signs of being harmed. Recently, Bianchi et al. showed how cisplatin (1 and 2 mg/kg twice weekly for 4 weeks) can cause the development of neuropathy, which is characterised by growth impairment, a decrease in SNCV, and a change in thermal threshold [141]. Mice and guinea pigs have also been employed as animal models for cisplatin-induced sensory neuropathy in addition to rats [142,143]. Low dosage models have the benefit of being less harmful to general health and have been shown to mimic neuropathy. Rodents treated with cisplatin exhibit behavioural, morphological, and electrophysiological alterations that closely resemble a variety of clinical neuropathy symptoms seen in people [144]. The loss in motor activity and strength shown in animal models, in contrast to human patients receiving cisplatin, has been a significant distinction between the human illness and the animal model [132,140,145].

Oxaliplatin-induced neuropathy:

The use of oxaliplatin, a third-generation novel platinum-derived chemical, in the treatment of advanced metastatic colorectal, ovarian, breast, and lung cancer has gained significant attention. Compared to prior platinum compounds, this current drug's toxicity profile is positive, meaning it is less harmful. Hematotoxic, nephrotoxic, and ototoxic effects. The toxicity it creates for peripheral sensory nerves, however, is unique. Oxaliplatin causes acute, reversible neurotoxicity (in up to 90% of cases). It is characterised by paresthesias in the hands,

feet, and peroral area as well as dysesthesia. Along with shortness of breath, the patients also have pharyngo-laryngo-dysesthesia [146]. Additionally, it has been seen to cause cumulative distal neurotoxicity, a kind of peripheral sensory symptomatic neuropathy marked by sensory ataxia, functional impairment, jaw pain, eye discomfort, ptosis, leg cramps, and changes in voice and vision [147]. Chronic peripheral oxaliplatin-induced neurotoxicity was documented by Avaletti et al. as altering electrophysiology [148]. According to their findings, the DRG's neuronal cell bodies are damaged by two cumulative dosages of oxaliplatin (36 and 48 mg/kg i.p.) and this results in a drop in SNCV. Jamieson et al. did not include any behavioural pain assessments in their description of a model of neuropathy that involved the repeated treatment of oxaliplatin for eight weeks in order to evaluate the histological changes to nerve cells [149]. Ling et al. used oxaliplatin at three distinct dosage regimens—1, 2, or 4 mg/kg intravenously—to present a novel animal model of nociceptive sensory neuropathy. Times a week for the previous four and a half weeks. Without any symptoms, mechanical allodynia, cold allodynia and hyperalgesia, heat thermal hyperalgesia, and allodynia have all been described with sign of motor function [150].

Taxanes-induced neuropathy models Paclitaxel-induced neuropathy:

Paclitaxel, a potent anti-neoplastic drug produced from the bark of the Pacific yew tree (Taxus brevifolia), is frequently used in chemotherapy regimens for the treatment of non-small cell lung, breast, ovarian, head, and neck malignancies. However, it has been noted that paclitaxel might cause sensory neuropathy, which is characterised by persistent, spontaneous burning pain in the distal extremities with tingling, numbness, mechanical allodynia, cold allodynia, and inventory distribution [152]. Sensory complaints often begin symmetrically in the feet; however they might occasionally strike both hands and feet at once. The uncomfortable side effects, which may include loss of vibratory feeling, deep tendon reflexes, and proprioceptive capacities, become more severe with repeated treatment. However, it has been shown that these functional anomalies might last for months, years, or even a lifetime with a reduced quality of life [152]. With paclitaxel alone, incidence rates of neuropathic pain have been shown to range from 22 to 100% at dosages of 250 mg/m2 and higher. Peripheral neuropathy has been linked to a variety of variables, including dosing regimen, overall therapy duration, total dose delivered, and co-administration of other chemotherapeutic drugs [153,154,155], and pre-existing diseases include alcohol misuse, diabetes, and peripheral nerve damage [134].

Low doses of paclitaxel (1 or 2 mg/kg i.p.) have been shown to induce pain syndrome in an animal model of neuropathy without endangering systemic health or impairing mice' motor function [156-158]. A peripheral neuropathy characterised by long-lasting tactile (mechanical) allodynia, endoneural edoema of the sciatic nerve, and cold allodynia has been observed following paclitaxel treatment on four alternate days (days 0, 2, 4, and 6; with a cumulative dosage of 4 or 8 mg/kg). On the fifth day of paclitaxel administration, changes in pain thresholds have been seen, and they endure for about 3 weeks after the final dosage. Rats treated with vincristine and paclitaxel exhibit strong mechanical and cold hypersensitivity but little to no heat hyperalgesia [156,157].

Two other dosing regimens, i.e.,16 mg/kg i.p., have also been devised for a higher dose model of paclitaxel-induced neuropathy. Paclitaxel is administered once a week for a total of 5 weeks at a cumulative dosage of 80 mg/kg or as a single injection at a dose of 32 mg/kg [158,159]. Rat models with larger cumulative doses (>15 mg/kg) than low dosage models have revealed thermal hypoalgesia, a sign of loss of thermal sensibility that is not present in low dose models. Another recent high dose paclitaxel model that induces large fibre sensory neuropathy (two doses of 18 mg/kg given over the course of three days, total cumulative dosage of 36 mg/kg) has also been created [159]. Other models have also been created that involve giving rats two doses of paclitaxel (18 mg/kg, i.v.) spaced by three days (for a total of 32 mg/kg) [180,181]. In these animals, neurophysiological modifications such as decreased sensory nerve conduction velocities and histological abnormalities have been observed [180,181]. Another animal has also shown that weekly intravenous injections of paclitaxel (5, 10, or 12.5 mg/kg) for 4 weeks can cause neuropathy [154]. Because these modifications are uncommon or non-existent in low dosage models of paclitaxel, loss of pain perception, morphological abnormalities, neurophysiological disturbances, and changes in motor function may be successfully examined in higher dose models [154,159,161,162].

Docetaxel-induced peripheral neuropathy:

Docetaxel, a semi-synthetic taxeme, is a common anti-neoplastic drug used to treat non-small cell lung, breast, and ovarian cancers. In a model of docetaxel-induced neuropathy, rats receive weekly intravenous injections of the drug (5, 10, or 12.5 mg/kg) to cause neuropathy. Rats given docetaxel have been observed to have slower tail nerve conduction velocities, altered temperature thresholds, and cutaneous nerve degeneration in the feeding pad [154,163].

Anti- HIV drugs-induced neuropathy:

The most successful form of treatment for AIDS is called highly active anti-retroviral therapy (HAART), which includes nucleoside reverse transcriptase inhibitors (NRTIs) such as ddC (zalcitabine), ddI (didanosine), and d4T (stavudine) as active ingredients. However, it has been seen that these medications exacerbate states of pain hypersensitivity brought on by HIV-1 infection and cause painful neuropathies [164-167]. Some NRTIs, such as ddC, are more powerful than ddI, which is more effective than d4T in generating sensory neurotoxicity, making them more likely to produce neuropathy than other NRTIs. Neither zidovudine nor abacavir, the other NRTIs, produce neuropathy [165]. According to Patterson et al., prolonged oral treatment of 415 mg/kg ddI twice day for 20 weeks causes a peripheral neuropathy that worsens after 15 weeks of dosage and is dose-dependent [168]. Additionally, Joseph et al. [169] constructed a brand-new model with a different dosage regimen and route of drug administration, namely ddC with doses of 25/50 mg/kg p.o. and ddC, ddI, and d4T with dose ranges of 10, 25, and 50 mg/kg intravenously. The maximum development of mechanical hyperalgesia is shown in

the nociceptive tests 5 days after ddC injection [169]. Mechanical hyperalgesia and allodynia, as well as thermal hyperalgesia, have been shown to be produced by oral doses of ddC (25 and 50 mg/kg) as well as i.v. doses of ddC, ddI, and d4T. Additionally, Bhangoo et al. created a unique animal model by giving ddC (25 mg/kg i.p.) as a single injection to induce mechanical allodynia [166]. Patients receiving large doses of ddI (30.4 mg/kg/day) for 12 weeks have similarities with peripheral neuropathy according to the Patterson et al. high oral dosage model [168, 170].

Disease-induced neuropathy models

Diabetes- induced neuropathy

Diabetic peripheral neuropathy (PDN) is a serious condition that frequently results in foot amputation. Clinical signs of neuropathy include higher temperature and vibration sensitivities, which eventually lead to sensory loss. Along with the loss of normal sensory function, patients also experience aberrant feelings such paresthesias, allodynia, hyperalgesia, and sudden pain [171]. The pancreatic b-cell toxins streptozotocin (STZ) and alloxan are utilised to create the most popular models for diabetic neuropathy [172,173]. However, in these models, animals also experience ketoacidosis, changes in lipid metabolism, and overall physical debility (lower growth and motor activity, lethargy, enlarged bladder, polyuria, and diarrhoea), in addition to hyperglycemia. Some of these symptoms make it more difficult to interpret the results of nociception investigations. The altered nociception measurements in diabetic rats caused by STZ have been attributed to overall debility rather than peripheral neuropathy. STZ has also been used to make mice develop diabetic neuropathy. The administration of a single dosage of STZ (200 mg/kg) for 4 weeks results in mice developing a high degree of hyperalgesia, according to research from our lab and those of other researchers [169,174,175].

A novel method for inducing diabetes has been devised, which involves injecting STZ (50 mg/kg) intravenously into the tail vein. It has been shown that an intravenous injection of STZ causes a notable early hyperglycaemia and glycosuria without a considerable amount of ketosis, weight loss, or overall physical weakness. Tactile allodynia, mechanical and thermal hyperalgesia, and their maximum development have all been shown to occur within 3 days. Additionally, it has been shown that the severity of behavioural changes is comparable to what was seen at 2- 3 weeks in rats given STZ subcutaneously [176].

The development of type I and type II transgenic animals that display PDN and other long-term diabetic complications. Goto-Kakizaki (GK) rats, Zucker diabetic fatty (ZDF) rats, Bio-breeding Zucker/Worcester (BBZDR/Wor) rats, db/db mice, and leptin-deficient (ob / ob) mice are some of the models used to study type II diabetes. GK rats display consistent, moderate hyperglycemia without obesity or ketosis [177]. Studies using a euglycemic hyperinsulinemic clamp have shown that these animals acquire insulin resistance in their peripheral tissues [178,179]. In GK rats, the neuropathic changes that occur with ageing have also been observed [180]. In 8-week-old hyperglycemic rats, the decrease in sensory and motor nerve conduction velocity (MNCV) has been documented. Thermal hyperalgesia that lasts at least 6 weeks has been seen in ZDF rats that are 8 weeks old. ZDF rats that are 10 weeks old have been proven to develop mechanical hyperalgesia [181]. Instead of type 2 diabetes, Goto-Kakizaki and Zucker obese rats serve as experimental models of the neuropathy of prediabetes because neither group exhibits overt fasting hyperglycemia [182] or does so only very late (40 weeks of age) after a decline in beta-cell function [182,183]. A slight impairment in MNCV has been seen in BBZDR/Wor-rats after 5 weeks of diabetes, but there has been no change in SNCV [184]. Additionally, it has been demonstrated that these rats lack sympathetic autonomic neuropathy and display milder axonal atrophy and fibre loss. [185]. Leptin binding is imperfect in db/db mice, which results in obesity, insulin resistance, hyperglycemia, and hypertriglyceridemia. It has been shown that diabetes individuals have fewer cutaneous nerve fibres on average and a lower average area density of nerve in the epidermis [186]. Morphometric analysis has shown that at the age of 6 months, sensory and motor neurons lack large, myelinated fibres and exhibit increasing axonal atrophy [187]. Obesity and mild type 2 diabetes are modelled in leptin-deficient (ob/ob) mice, who also develop moderate hyperglycemia, hyperinsulinemia, and obesity [188,189]. These animals have been shown to develop PDN (11-week-old), which is characterised by sensory deficits as well as MNCV deficits, thermal hypoalgesia, tactile allodynia, and epidermal sensory fibre loss—features that are typical in diabetic people [190,191]. Thermal hypoalgesia, a syndrome seen in humans with diabetic neuropathy, has been demonstrated in these animals [171]. However, persistent thermal hyperalgesia, which is a temporary symptom of neuropathy in humans, has been shown in other models, including BBZDR/Wor-rats and ZDF rats [181,182,192,193]. Considering this, the model is a useful example of an animal PDN for type 2 diabetes and obesity.

Hyperglycaemia first manifests in the non-obese diabetic (NOD) mouse, a type II diabetes model, between 12 and 30 weeks of age. Very little research has been done to examine the complications of diabetes since they often develop at a late and unknown age and require more intense therapy, such as daily exogenous insulin delivery. According to studies, 18-week-old NOD mice exhibit thermal hypoalgesia [194]. Additionally, it has been demonstrated that diabetic NOD mice experience substantial hyperalgesia that begins to manifest at 8 to 10 weeks along with their diabetes and can endure for up to 32 weeks [195]. A close replica of type 1 diabetes in humans, the bio-breeding/Worcester rat (BB/Wor rat) experiences hyperglycemia and insulinopenia around the time of 12 weeks of age. Beginning at the age of 4 months, neuropathy symptoms such as hyperalgesia, a decrease in the number of unmyelinated fibers, mean axonal size, and decreased nerve conduction velocity appear [196- 198]. After 5 weeks of diabetes, there is a higher decline in MNCV than SNCV in BB/Wor-rats. The nodal and paranodal axonal enlargement in myelinated fibres, which causes perturbed axonal transport and gradual axonal atrophy, is one of the earliest noticeable alterations [184].

Cancer pain models

Patients who are suffering from advanced cancer pain have serious challenges, and the causes of cancer pain are yet unknown. Bone cancer pain has been modelled in a variety of animal models of cancer pain [199-201], neuropathic cancer pain [202], and skin cancer

pain [203]. The specific pharmacological and neurochemical characteristics of cancer pain have been shown in these models, pointing to the participation of inflammatory, neuropathic, and tumorigenic elements in the pathophysiology of pain [204].

Bone cancer pain models.

One of the most frequent cancer-related aches is bone cancer pain, which can originate from bone cancer or spread from breast, prostate, ovarian, or lung malignancies [205].

Mouse femur bone cancer pain.

Initially, Schweich et al. created a model based on the painful osteosarcoma that was produced when osteolytic fibrosarcoma (NCTC 2472) cells were injected into the femur of C3H/HeJ mice. In this model, the patellar ligament is severed, and the condyles of the distal femur are exposed by a 1 cm superficial incision in the hind leg [200]. In order to create a cavity for the injection of the cells, a 23-gauge needle is then inserted at the level of the intercondylar notch and the intramedullary canal of the femur. Approximately 2.5 106 osteolytic murine sarcoma cells, NCTC2472, are injected into the bone cavity in a 20microliter volume [200,207-209]. Cancer-induced bone loss and osteoclastogenesis have been shown to occur within 5 days following sarcoma injection, resulting in both spontaneous (nocifensive behaviour, spontaneous flinching) and prompted pain (palpation-evoked flinching) [210,211].

Calcaneus bone cancer pain (CBC).

The only difference between this model and the prior model is that NCTC2472 cells are injected into the calcaneus bone [201,212]. Osteolysis, induced pain (mechanical and cold allodynia), and spontaneous pain (paw licking) have all been shown to start 6 days after implantation and persist for at least 16 days. Additionally, it has been proven that the spontaneous activity and heat sensitivity of C-fibers are related to the development of tumours [213].

Tibial bone cancer pain:

In this model, rats' tibial bones are injected with rat mammary gland carcinoma cells (MRMT-1) [214,215]. Within 10 to 12 days following the injection of tumour cells, bone degradation, the onset of allodynia, and mechanical hyperalgesia have all been seen. Mechanical hyperalgesia and spinal nociceptive neuron sensitization are brought on by the injection of these MRMT-1 cells in rats, which results in the formation of bone tumours. Another model has shown that intratibial injection of NCTC 2472 cells causes an osteosarcoma and a decrease in heat responsiveness within the first two weeks following cell implantation. The fourth and fifth weeks following the implantation of NCTC 2472 cells, on the other hand, have been associated with an increase in nociceptive heat responsiveness [199].

Humerus bone cancer pain (CBC).

Bone cancer frequently exhibits movement-related hyperalgesia, also referred to clinically as a particular sort of "breakthrough pain." Finding the peripheral and central processes underlying the pain that comes along with bone metastases may be made easier with the establishment of an animal model of movement-related hyperalgesia. Additionally, it could be useful in separating it from the discomfort brought on by muscle inflammation. Injecting NCTC2472 cells into the humerus' medullary cavity has been used to create an animal model of this, which results in forelimb hyperalgesia but not evident mechanical hyperalgesia in the forepaw. The histological analysis shows a direct link between behavioural hyperalgesia and tumour growth-induced bone damage [216,217].

Neuropathic cancer pain model.

To create a mouse model of neuropathic cancer pain, a cancerous tumour was grown close to the sciatic nerve. The right sciatic nerve is exposed at the level of the gluteus while under anaesthesia, and ascites containing 50,000 tumour cells (Meth A sarcoma cells) are injected near the sciatic nerve. Thermal hyperalgesia and mechanical allodynia gradually develop in the ipsilateral hind paw because of a tumor' s growth compressing the sciatic nerve over time. The raising of the paw is one of the reported indications of spontaneous pain. Thermal hyperalgesia and symptoms of spontaneous pain continue, but subsequent tumour development reverses the mechanical hypersensitivity and results in mechanical hyposensitivity. Histologically, both myelinated and unmyelinated axons are gradually damaged as a result of the tumor' s steady compression [202,208].

Skin cancer pain model.

A particularly intrusive kind of Lung metastasis and cancer pain have been developed using B16 melanoma, or B16-BL6 cells. These melanoma cells (2 105 cells, 20 lL) are subcutaneously injected into the mouse's unilateral hind paw [203,218]. It has been documented that an orthotropic injection of B16-BL6 melanoma cells into the hind paw causes moderate and significant hyperalgesia on days 7 to 10 (early phase) and day 14 (late phase) post-inoculation, respectively [203].

Human immunodeficiency virus (HIV)-induced neuropathy.

Among the most common presentation of chronic pain in patients infected with HIV is distal symmetrical polyneuropathy characterized by painful sensory abnormalities, which may affect up to 30% of AIDS patients [219,220]. The exterior envelope protein of HIV-1, gp120, is thought to bind to the chemokine receptors CXCR4 and CCR5 that are found on neurons and glial cells, mediating its apparent interactions with the neurological system [165] that results in neurotoxicity [220] and peripheral axonal damage [221]. The effects of HIV infection-induced neuropathy have been duplicated in rats by anaesthetizing the animals and isolating the left sciatic nerve without harming the perineurium. The HIV-1 envelope protein gp120 is saturated with either 20 or 400 ng in the oxidised cellulose (oxycel), which is employed as a carrier matrix to deliver proteins directly to the sciatic nerve. The muscle layer is closed, and the oxycel containing viral glycoprotein is loosely wrapped around the sciatic nerve, 2-3 mm proximal to the trifurcation. Peripheral neuropathy that is chronically painful is caused by epineural exposure to the HIV-1 envelope protein gp120. Following gp 120 exposures, allodynia and hyperalgesia have been shown to emerge within 1-3 days and last for a considerable amount of time [222,223].

Post-herpetic neuralgia model

The extremely contagious neurotropic virus varicella zoster (VZV) initially infects individuals with varicella (chickenpox), and then establishes a latent infection by travelling retrogradely down sensory neurons' axons. in the peripheral nerve system's sensory ganglia [224]. Viral reactivation often happens because of cellular immunity ageing and manifests as acute herpes zoster (AHZ) (shingles) [224,225]. The development of PHN, a neuropathic pain condition marked by persistent pain and different degrees of sensory deficiencies at least three months following healing of skin lesions, complicates the recovery from AHZ [226]. Sadzot-Delvaux et al. developed the first in vivo animal model of latent VZV infection, which involved injecting infected Mewo cells with virus subcutaneously into the foot of healthy adult rats. In this rat model, the presence of viral particles in the DRG and the humoral immune response to VZV have both been characterised [227,228]. Based on this paradigm, a novel model has been created with typical sensory alterations in rats that are comparable to those seen in PHN patients [229]. The model calls for spreading VZV on CV-1 cells, which are kidney fibroblasts from an African green monkey, and then collecting the virus-infected cells (with an 80% cytopathic impact). Rats are then put to sleep, and a subcutaneous injection of virally infected cells (4 106 infected cells; 50 lL) is administered to the left globous footpad. According to reports, there are noticeable behavioural changes, such as mechanical allodynia and hyperalgesia, that start to manifest three days after injection, peak between 10 and 21 days later, last for more than 60 days, and then go away after 100 days [229,230].

Herpes simplex virus-induced neuropathy.

The type 1 herpes simplex virus (HSV-1) is a neurotropic virus that can cause following infection, latent in the sensory ganglia. Following infiltration into the host, the virus proceeds through initial replication in the skin or mucosa before being transported down axons to reach the peripheral terminals of sensory neurons. According to their clinical complaints, HSV-infected individuals experience paraesthesia, dysesthesia, hypoalgesia, tingling, and formication [231]. Prior to eruption, there is discomfort, and some patients continue to experience pain in the form of PHN long after the vesicles have disappeared [231]. HSV-1 (1 106 plaque-forming units) is injected into the shin of the hind paw to mimic the symptoms of PHN in mice. On day 5, the hind paw on the infected side shows the onset of allodynia and hyperalgesia, which last for at least 8 days. In addition, HSV-1 DNA was found in the DRG from days 2 to 8 after the vaccination, with the highest impact occurring on day 5 [232,233].

Non-viral model of PHN.

The drawbacks of using virally infected cells to create an animal model of PHN include the need for specific, separate chambers for the virus to grow as well as the development of tissue inflammation, skin sores, and paralysis because of the virus spreading to the central nervous system [232,233]. Resiniferous toxin (RTX), an extremely potent TRPV1 agonist, has been reported to produce long-lasting changes in adult rats' mechanical and thermal sensitivity, simulating the distinct clinical feature of PHN. As a result, a new animal model has been created to overcome these limitations [234,235]. It has been shown that a single i.p. injection of RTX (200 lg/kg) decreases heat sensitivity but causes a significant and long-lasting increase in mechanical sensitivity. Capsaicin-sensitive afferent neuron loss has been suggested as the cause of RTX's reduced thermal sensitivity. On the other hand, myelinated afferent fibre injury and their aberrant sprouting into the spinal lamina II have been connected to the delayed and prolonged tactile allodynia in RTX-treated rats [236].

Miscellaneous models

Chronic ethanol consumption/ withdrawal-induced neuropathy:

Long-term alcohol use has been shown to cause small-fiber painful neuropathy, also known as dying back neuropathy, which is characterised by distal axonal degeneration. Alcohol use initially causes some analgesia, but with time, induction of pain overcomes analgesia and causes neuropathic pain syndrome, which has been characterised as feeling "like pulling skin from the bones." Rats are given 6.5% ethanol daily for a period of 12 weeks to create the animal models of chronic alcohol intake and withdrawal-induced neuropathy [236,237], based on the guidelines for feeding rats a diet containing alcohol [236,238]. The liquid ethanol diet is progressively increased for the rats, as follows: from the first to third day, 2.5 w/v%; from the fourth to sixth day, 4 w/v%; from the seventh to 16th day, 4.5 w/v%; and from the seventeenth to the seventieth day, 5 w/v%. Rats are given a liquid meal containing ethanol on a decreasing ethanol dose schedule, with 2.5 w/v% ethanol for the first day, 1.25 w/v% ethanol for the second day, and 0 w/v% ethanol for the third day, after receiving ethanol therapy for 70 days. The liquid diets are then replaced with regular meals [239,240]. There is evidence that the mechanical hyperalgesia starts to develop after 12 weeks of alcohol use and continues long after ethanol abstinence [236,237,241].

Pyridoxine (vitamin B6)- induced neuropathy

Numerous animal species, including dogs, have exhibited the sensory neuropathy associated with pyridoxine poisoning that occurs in humans. It has been proven that giving pyridoxine orally for 112 days at a level between 50 and 300 mg/kg/day causes sensory anomalies indicative of neuropathy [242-244]. These models are run over a lengthy period; however, they are based on extremely high pyridoxine dosages. In the more recent model, it has been demonstrated that giving dogs 150 mg/kg of pyridoxine once a day for seven days causes them to exhibit signs of neuropathy [245]. Rat models of neuropathy brought on by pyridoxine have also been created [246,247]. In rat models, three intraperitoneal dosage regimens with short-term/high doses of 1200 mg/kg/day for 1–15 days have been used [248,249], a middle dosage of 600 mg/kg/day for 1 to 15 days [246,249], additionally long-term/low dosage, 100–300 mg/kg/day for as long as 12 weeks [247-249]. At low and intermediate levels, a reversible sensory nerve axonopathy has been characterised as the secondary cause of neuropathy, while at high doses, an irreversible sensory ganglion neuropathy [244,246,247]. With i.p. treatment of pyridoxine (400

mg/kg twice daily for 14 days), neuropathy may be induced in rats using the intermediate dosage technique [250]. During the first week, no evidence of pyridoxine-induced functional impairment has been noted. The functional deficiencies manifest in all four limbs during the second week, impairing coordination. The functional deficits become more noticeable [250].

Trigeminal neuralgia models

Trigeminal neuralgia is a severe kind of chronic pain condition marked by paroxysmal pain that feels like an electrical shock for a limited period [251]. The trigger zone, which is typically on the face or in the oral cavity, is stimulated gently by touch to cause the pain, which is typically unilateral [252]. Due to various etiologies, the disease's pain may be classified as central or peripheral. Patients with multiple sclerosis frequently get trigeminal neuralgia [253], and the central pain is the kind of discomfort reported in multiple sclerosis [254]. The stereotaxic frame is attached to the sedated rats, and a tiny hole in the skull is created before a guide cannula (21 gauge) is inserted into the left trigeminal ganglion. The trigeminal ganglion is then compressed by injecting 4% agar solution through a stainless-steel injector (24 gauge), extending 1 mm above the tip of a guide cannula, into the dorsal side of the left trigeminal ganglion. The 10 lL of agar solution is progressively pumped into the injector over the course of 5 s, and it is then kept in place for 10 min before being removed. The trigeminal ganglion is compressed without suffering any damage when the agar is applied to its dorsal surface [255,256]. Mirror-image mechanical allodynia has been seen to result from compression of the trigeminal ganglion. The reactions to mechanical stimulation of the face, particularly the vibrissa pad, including the mouth angle or the mandibular region, have dramatically increased, and this is one of the most noticeable behavioural alterations that occur after the compression of the trigeminal ganglion [256].

Secondary trigeminal neuralgia (STN) or reflex sympathetic dystrophy are two different diagnoses for persistent neuropathic pain syndromes that can occasionally be brought on by trauma, dental procedures, and orofacial surgery [257]. STN has been characterised as significantly different from idiopathic trigeminal neuralgia, even though the two conditions share some characteristics. The development of heat-hyperalgesia has been seen in an experimental rat model of secondary trigeminal neuropathic pain caused by a CCI to the infra-orbital nerve (CCI-ION) [258]. Intraoral incisions are done while the patient is under anaesthesia, preserving the vibrissae and snout hair. Just beyond the first tooth, a 1-cm-long incision is made along the gingivobuccal edge. One infra-orbital nerve (ION), which is about 0.5 cm long and covered with adherent tissue, is released, and two ligatures (4.0 chromic gut) are wrapped loosely around it to cause neuropathic pain resembling secondary trigeminal neuralgia. Dynamic mechanical allodynia, which is clinically more applicable than static allodynia, is one benefit of this model of trigeminal neuropathic pain [259].

Orofacial pain models

Orofacial discomfort has been studied in a variety of animals to better understand the underlying processes and to shed light on potential treatment options. Eisenberg and colleagues established an experimental model of orofacial pain in which rats' whiskers were subcutaneously injected with formalin, causing a biphasic grooming response. Rats exhibit a reaction, which is a nociceptive activity [260]. A biphasic grooming response, which is a nociceptive activity in rats, is produced by subcutaneous formalin injection at the base of the whiskers of rats. A mouse model that involves injecting carrageenan under the skin over the right maxilla has been developed [261,262].

Acrylamide-induced neuropathy model

Acrylamide is a well-known water-soluble vinyl monomer with several industrial uses, including the manufacturing of polymers (polyacrylamide), the processing of ores, the creation of dyes and fibres, and the purifying of paper and water [263]. The creation of acrylamide from asparagine, which is contained in potato chips and French fries when cooked at high temperatures, increases the amount of acrylamide that humans are exposed to [264-266]. Both in humans and animals, acrylamide has been shown to have neurotoxic effects on both the peripheral and central nervous systems [263]. Flaccid paralysis and ataxia are symptoms of acrylamide-induced behavioural neurotoxicity, a central-peripheral distal (dying back type) axonopathy that indicates axon degeneration [266]. Using various dosages of acrylamide, a mouse model of acrylamide-induced neuropathic pain has been created [263,266,267]. It has been demonstrated that neuropathy symptoms can be induced by administering acrylamide i.p. three days a week for eight weeks at doses between 20, and 40 mg/kg [267]. Rats exposed to lesser doses acquire an unstable gait pattern with hind limb abduction and external rotation, whereas rats subjected to larger doses exhibit foot dragging when walking, foot splay, bent toes, and obvious ataxia [266]. In the sciatic nerve and dorsal root ganglion cells of rats, morphological changes have been documented at higher doses (>40 mg/kg) [263].

Monoiodoacetate model of osteoarthritis

Numerous histological characteristics of the clinical state are shared by the osteoarthritis-related joint degradation shown in the rat monoiodoacetate (MIA) model. The model has been extensively utilised to study the biology of osteoarthritis pain and for preclinical screening of analgesic drugs because to the associated pain phenomenology. the pathophysiological effects of MIA utilised at low (1 mg) or high (2 mg) doses were examined. ATF-3, a sensitive marker for peripheral neuron stress/injury, was primarily expressed in small and large diameter DRG cell profiles at levels L4 and 5, as opposed to L3 (levels mostly by neurons innervating the hindpaw). ATF-3 signal in rats treated with 1 mg of MIA compared well to those treated with 2 mg at the 7-day timepoint. In addition to producing spinal cord dorsal and ventral horn microgliosis, 2 mg of intra-articular MIA, but not 1 mg, was linked to a substantial decrease in intra-epidermal nerve fibre density in the skin of the plantar hindpaw. Compared to the 1 mg treatment, the 2 mg treatment significantly increased the hindpaw's mechanical pain-related hypersensitivity. Weight bearing asymmetry and cold hypersensitivity were side effects of MIA therapy that were identical at both dosages. Pregabalin substantially decreased deep dorsal horn evoked neuronal responses in rats treated with 2 mg MIA,

but this effect was greatly diminished or nonexistent in animals given with 1 mg or sham. These findings show that intra-articular 2 mg MIA induces severe axonal damage to DRG cells, including those innervating targets outside of the knee joint, such as the skin on the back of the paw. Studies employing this paradigm need to be interpreted with this strong neuropathic component in mind, especially at dosages higher than 1 mg MIA [268,269].

Conclusion

Numerous animal models of neuropathic pain have been developed because neuropathic pain has numerous etiologies. Models based on peripheral nerve damage caused by ligation have been used increasingly often. However, models based on transection of peripheral nerve branching have clear benefits and are used more frequently today. The preferred models for SCI are excitotoxin-induced SCI and spinal hemisection are the models of choice for understanding central pain mechanisms. In addition, other research groups have used the pain models caused by chemotherapeutic drugs, diabetes, HIV, alcoholism, and others to comprehend the pathogenesis and control the pain that has different respective etiologies in clinical settings and that reflects in new drug discovery for neuropathic pain in humans.

Acknowledgements

The study is self-funded and there are no funding sources. It is declared that all authors have no competing interests. Protocol and procedures employed were ethically reviewed and approved.

References

1. Mitchell SW (1872) Injuries of nerves and their consequences. JB Lippincott Philadelphia.
2. Woolf CJ, Mannion RJ (1999) Neuropathic pain: aetiology, symptoms, mechanisms, and management. Lancet 353(9168): 1959-1964.
3. Schmader KE (2002) Epidemiology and impact on quality of life of postherpetic neuralgia and painful diabetic neuropathy. Clin J Pain 18(6): 350-354.
4. Werhagen L, Budh CN, Hultling C, Molander C (2004) Neuropathic pain after traumatic spinal cord injury relations to gender, spinal level, completeness, and age at the time of injury. Spinal Cord 42(12): 665-673.
5. Perkins FM, Kehlet H (2000) Chronic pain as an outcome of surgery. A review of predictive factors. Anesthesiology 93(4): 1123-1133.
6. Wall PD, Gutnick M (1974) Properties of afferent nerve impulses originating from a neuroma. Nature 248(5415): 740-743.
7. Wall PD, Devor M, Inbal R (1979) Autotomy following peripheral nerve lesions: experimental anaesthesia dolorosa. Pain 7(2): 103-113.
8. Devor M, Wall PD (1976) Type of sensory nerve fibre sprouting to form a neuroma. Nature 262 (5570): 705-708.
9. Jaggi AS, Jain V, Singh N, (2011) Animal models of neuropathic pain. Fundamental clinical pharmacology 25(1) pp.1-28.
10. Wall PD, Scadding JW, Tonikiewicz MM (1979) The production and prevention of experimental anesthesia dolorosa. Pain 6 (2): 175-182.
11. Zeltser R, Beilin B, Zaslansky R, Seltzer Z (2000) Comparison of autotomy behavior induced in rats by various clinically used neurectomy methods. Pain 89(1): 19-24.
12. Kauppila T (1998) Correlation between autotomy-behavior and current theories of neuropathic pain. Neurosci Biobehav Rev 23(1): 111-129.
13. Riopelle JM (1992) The ethics of using animal models to study treatment of phantom pain. Anaesthesiology 76(6): 1069- 1071.
14. Bennett GJ, Xie YK (1988) A peripheral mononeuropathy in rat that produces disorders of pain sensation like those seen in man. Pain 33(1): 87-107.
15. Muthuraman A, Jaggi AS, Singh N, Singh D (2008) Ameliorative effects of amiloride and pralidoxime in chronic constriction injury and vincristine-induced painful neuropathy in rats. Eur J Pharmacol 587(1-3): 104-111.
16. Martucci C, Trovato AE, Costa B (2008) The purinergic antagonist PPADS reduces pain related behaviours and interleukin-1 beta, interleukin-6, iNOS and nNOS overproduction in central and peripheral nervous system after peripheral neuropathy in mice. Pain 137(1): 81- 95.
17. Sacerdote P, Franchi S, Trovato AE, Valsecchi AE, Panerai AE, et al. (2008) Transient early expression of TNF-a sciatic nerve and dorsal root ganglia in a mouse model of painful peripheral neuropathy. Neurosci. Lett. 436(2): 210-213.
18. De Vry J, Kuhl E, Franken-Kunkel P, Eckel G (2004) Pharmacological characterization of the chronic constriction injury model of neuropathic pain. Eur J Pharmacol 491(2-3): 137-148.
19. Dowdall T, Robinson I, Meert TF (2005) Comparison of five different rat models of peripheral nerve injury. Pharmacol Biochem Behav 80(1): 93-108.
20. Carlton SM, Dougherty PM, Pover CM, Coggeshall RE (1991) Neuroma formation and numbers of axons in a rat model of experimental peripheral neuropathy. Neurosci Lett 131(1): 88-92.
21. Gabay E, Tal M (2004) Pain behavior and nerve electrophysiology in the CCI model of neuropathic pain. Pain 110(1-2): 354- 360.
22. Nakamura S, Atsuta Y (2006) The effects of experimental neurolysis on ectopic firing in a rat chronic constriction nerve injury model. J Hand Surg Am 31(1): 35-39.
23. Jaggi AS, Jain V, Singh N (2011) Animal models of neuropathic pain. Fundamental clinical pharmacology 25(1) pp.1-28.
24. Ro LS, Jacobs JM (1993) The role of the saphenous nerve in experimental sciatic nerve mononeuropathy produced by loose ligatures: a behavioural study. Pain 52(3): 359-369.
25. Seltzer Z, Dubner R, Shir Y (1990) A novel behavioural model of neuropathic pain disorders produced in rats by partial sciatic nerve injury. Pain 43(2): 205-218.
26. Kim KJ, Yoon YW, Chung JM (1997) Comparison of three rodent neuropathic pain models. Exp. Brain Res 113(2): 200- 206.
27. Xu M, Bruchas MR, Ippolito DL, Gendron L, Chavkin C (2007) Sciatic nerve ligation-induced proliferation of spinal cord astrocytes is mediated by l opioid activation of p38mitogen-activated protein kinase. J Neurosci 27(10): 2570-2581.
28. Mitchell VA, White DM, Cousins MJ (1999) The long-term effect of epidural administration of butamben suspension on nerve injury-induced allodynia in rats. Anesth Analg 89(4): 989-994.
29. Malmberg AB, Basbaum AI (1998) Partial sciatic nerve injury in the mouse as a model of neuropathic pain: behavioral and neuroanatomical correlates. Pain 76 (1-2): 215-222.
30. Yoon YW, Lee DH, Lee BH, Chung K, Chung JM (1999) Different strains of rats show different levels of neuropathic pain behaviors. Exp Brain Res 129(2): 167-171.
31. Bennett GJ (1993) An animal model of neuropathic pain: a review. Muscle Nerve 16(10): 1040-1048.
32. Seltzer Z (1995) The relevance of animal neuropathy models for chronic pain in humans. Sem. Neurosci 7: 211-219.

33. Kim SH, Chung JM (1992) An experimental model for peripheral neuropathy produced by segmental spinal nerve ligation in the rat. Pain 50(3): 355-363.

34. Lin CS, Tsaur ML, Chen CC, et al. (2007) Chronic intrathecal infusion of minocycline prevents the development of spinalnerve ligation-induced pain in rats. Reg Anesth Pain Med 32(3): 209-216.

35. Choi Y, Yoon YW, Na HS, Kim SH, Chung JM (1994) Behavioural signs of ongoing pain and cold allodynia in a rat model of neuropathic pain. Pain 59(3): 369-376.

36. LaBuda CJ, Little PJ, (2005) Pharmacological evaluation of the selective spinal nerve ligation model of neuropathic pain in the rat. J Neurosci Methods 144(2): 175-181.

37. Kinnman E, Levine JD (1995) Sensory and sympathetic contributions to nerve injury-induced sensory abnormalities in the rat. Neuroscience 64(3): 751-767.

38. Xie J, Yoon YW, Yom SS, Chung JM (1995) Norepinephrine rekindles mechanical allodynia in sympathectomized neuropathic rat. Analgesia 1: 107-113.

39. Lee BH, Yoon YW, Chung K, Chung JM (1998) Comparison of sympathetic sprouting in sensory ganglia in three animal models of neuropathic pain. Exp Brain Res 120(4): 432- 438.

40. Carlton SM, Lekan HA, Kim SH, Chung JM (1994) Behavioral manifestations of an experimental model for peripheral neuropathy produced by spinal nerve ligation in the primate. Pain 56(2): 155-166.

41. Shields SD, Eckert III WA, Basbaum AI (2003) Spared nerve injury model of neuropathic pain in the mouse: a behavioral and anatomic analysis. The Journal of Pain 4(8) pp.465-470.

42. Pertin M, Gosselin RD, Decosterd I (2012) The spared nerve injury model of neuropathic pain. Methods Mol Biol 851: 205-12.

43. Decosterd I, Woolf CJ (2000) Spared nerve injury: an animal model of persistent peripheral neuropathic pain. Pain 87(2): 149-158.

44. Bourquin AF, Su¨veges M, Pertin M, et al. (2006) Assessment and analysis of mechanical allodynia-like behavior induced by spared nerve injury (SNI) in the mouse. Pain 122(1-2): 14.e1-14.e14.

45. Kohno T, Moore KA, Baba H, Woolf CJ (2003) Peripheral nerve injury alters excitatory synaptic transmission in lamina II of the rat dorsal horn. J Physiol 548: 131-138.

46. Baliki M, Calvo O, Chialvo DR, Apkarian AV (2005) Spared nerve injury rats exhibit thermal hyperalgesia on an automated operant dynamic thermal escape Task. Mol Pain 1: 18.

47. Pertin M, Allchorne AJ, Beggah AT, Woolf CJ, Decosterd I (2007) Delayed sympathetic dependence in the spared nerve injury (SNI) model of neuropathic pain. Mol Pain 3: 21.

48. Shields SD, Eckert WA, Basbaum AI (2003) Spared nerve injury model of neuropathic pain in the mouse: a behavioral and anatomic analysis. J Pain 4(8): 465-470.

49. Lee BH, Won R, Baik EJ, Lee SH, Moon CH (2000) An animal model of neuropathic pain employing injury to the sciatic nerve branches. Neuroreport 1(4): 657-661.

50. Jain V, Jaggi AS, Singh N (2009) Ameliorative potential of rosiglitazone in tibial and sural nerve transection-induced painful neuropathy in rats. Pharmacol Res 59(6): 385- 392.

51. Dowdall T, Meert TF (2005) Behavioural evaluation of symptoms of allodynia and hyperalgesia in rats with a tibial and sural nerve transection. J Neuropathic Pain Symptom Palliation 1(1): 29-37.

52. Unal-Cevik I, Oaklander AL (2011) Comparing Partial and Total Tibial-Nerve Axotomy: Long-Term Effects on Prevalence and Location of Evoked Pain Behaviors. Pain Practice 11(2): 109-119.

53. Vadakkan KI, Jia YH, Zhuo M (2005) A behavioral model of neuropathic pain induced by ligation of the common peroneal nerve in mice. J Pain 6(11): 747-756.

54. Omori Y, Kagaya K, Enomoto R, Sasaki A, Andoh T, et al. (2009) A mouse model of sural nerve injury-induced neuropathy: gabapentin inhibits pain-related behaviors and the hyperactivity of wide-dynamic range neurons in the dorsal horn. Journal of pharmacological sciences 109(4): 532-539.

55. Vadakkan KI, Jia YH, Zhuo M (2005) A behavioral model of neuropathic pain induced by ligation of the common peroneal nerve in mice. The Journal of Pain 6(11): 747-756.

56. Wagner R, DeLeo JA, Coombs DW, Willenbring S, Fromm C (1993) Spinal dynorphin immunoreactivity increases bilaterally in a neuropathic pain model. Brain Res 629(2): 323-326.

57. DeLeo JA, Coombs DW, Willenbring S, et al. (1994) Characterization of a neuropathic pain model: sciatic cryoneurolysis in the rat. Pain 56(1): 9-16.

58. Colburn RW, Rickman AJ, DeLeo JA (1999) The effect of site and type of nerve injury on spinal glial activation and neuropathic pain behavior. Exp Neurol 157(2): 289-304.

59. DeLeo JA, Coombs DW, Willenbring S, Colburn RW, Fromm C, et al. (1994) Characterization of a neuropathic pain model: sciatic cryoneurolysis in the rat. Pain 56(1): 9-16.

60. Na HS, Han JS, Ko KH, Hong SK (1994) A behavioural model for peripheral neuropathy produced in rat's tail by inferior caudal trunk injury. Neurosci Lett 177(1-2): 50-52.

61. Sung B, Na HS, Kim YI, et al. (1998) Supraspinal involvement in the production of mechanical allodynia by spinal nerve injury in rats. Neurosci Lett 246(2): 117-119.

62. Back SK, Lee J, Hong SK, Na HS (2006) Loss of spinal l-opioid receptor is associated with mechanical allodynia in a rat model of peripheral neuropathy. Pain 123(1-2): 117-126.

63. Sung B, Loh HH, Wei LN (2000) Association of kappa opioid receptor mRNA upregulation in dorsal root ganglia with mechanical allodynia in mice following nerve injury. Neurosci Lett 291(3): 163-166.

64. Back SK, Sung B, Hong SK, Na HS (2002) A mouse model for peripheral neuropathy produced by a partial injury of the nerve supplying the tail. Neurosci Lett 322(3): 153- 156.

65. Said G, Hontebeyrie Joskowicz M (1992) Nerve lesions induced by macrophage activation. Res. Immunol. 143(6): 589-599.

66. Chacur M, Milligan ED, Gazda LS (2001) A new model of sciatic inflammatory neuritis (SIN): induction of unilateral and bilateral mechanical allodynia following acute unilateral peri sciatic immune activation in rats. Pain 94(4): 231-244.

67. Gazda LS, Milligan ED, Hansen MK (2001) Sciatic inflammatory neuritis (SIN): behavioral allodynia is paralleled by peri-sciatic proinflammatory cytokine and superoxide production. J. Peripher Nerv Syst. 6(3): 111-129.

68. Wagner R, Myers RR (1996) Endoneurial injection of TNF-alpha produces neuropathic pain behaviors Neuroreport 7(18): 2897-2901.

69. Wang H, Bloom O, Zhang M (1999) HMG-1 as a later mediator of endotoxin lethality in mice. Science 285(5425): 248-251.

70. Eliav E, Herzberg U, Ruda MA, Bennett GJ (1999) Neuropathic pain from an experimental neuritis of the rat sciatic nerve. Pain 83(2): 169-182.

71. Maleki J, LeBel AA, Bennett GJ, Schwartzman RJ (2000) Patterns of spread in complex regional pain syndrome, type I (reflex sympathetic dystrophy). Pain 88(3): 259-266.

72. Shir Y, Seltzer Z (1991) Effects of sympathectomy in a model of causalgiform pain produced by partial sciatic nerve injury in rats. Pain 45(3): 309-320.

73. Milligan ED, Maier SF, Watkins LR (2004) Sciatic Inflammatory Neuropathy in the Rat. In Pain Research, Humana Press, pp. 67-89.

74. Mosconi T, Kruger L (1996) Fixed-diameter polyethylene cuffs applied to the rat sciatic nerve induce a painful neuropathy: ultrastructural morphometric analysis of axonal alterations. Pain 64(1): 37-57.

75. Pitcher GM, Ritchie J, Henry JL (1999) Nerve constriction in the rat: model of neuropathic, surgical and central pain. Pain 83(1): 37-46.

76. Coull JA, Boudreau D, Bachand K (2003) Trans-synaptic shift in anion gradient in spinal lamina I neurons as a mechanism of neuropathic pain. Nature 424(6951): 938-942.

77. Benbouzid M, Pallage V, Rajalu M (2008) Sciatic nerve cuffing in mice: a model of sustained neuropathic pain. Eur J Pain 12(5): 591-599.

78. Benbouzid M, Gave´riaux Ruff C, Yalcin I, et al. (2008) Delta-opioid receptors are critical for tricylic antidepressant treatment of neuropathic allodynia. Biol Psychiatry 63(6): 633-636.

79. Coull JA, Beggs S, Boudreau D, et al. (2005) BDNF from microglia causes the shift in neuronal anion gradient underlying neuropathic pain. Nature 438(7070): 1017-1021.

80. Yalcin I, Choucair Jaafar N, Benbouzid M, et al. (2009) Beta (2) adrenoceptors are critical for antidepressant treatment of neuropathic pain. Ann. Neurol. 65(2): 218-225.

81. Gazelius B, Cui JG, Svensson M, Meyerson B, Linderoth B (1996) Photochemically induced ischaemic lesion of the rat sciatic nerve. A novel method providing high incidence of mononeuropathy. Neuroreport 7(15-17): 2619-2623.

82. Kupers R, Yu W, Persson JKE, Xu XJ, Wiesenfeld Hallin Z (1998) Photochemically-induced ischemia of the rat sciatic nerve produces a dose-dependent and highly reproducible mechanical, heat and cold allodynia, and signs of spontaneous pain. Pain 76(1-2): 45-59.

83. Hao JX, Blakeman KH, Yu W, Hultenby K, Xu XJ, et al. (2000) Development of a mouse model of neuropathic pain following photochemically induced ischemia in the sciatic nerve. Exp Neurol 163(1): 231- 238.

84. Myers RR, James HE, Powell HC (1985) Laser injury of peripheral nerve: a model for focal endoneurial damage. J Neurol Neurosurg Psychiatry 48(12): 1265-1268.

85. Chiang HY, Chen CT, Chien HF, Hsieh ST (2005) Skin denervation, neuropathology, and neuropathic pain in a laser-induced focal neuropathy. Neurobiol Dis 18(1): 40-53.

86. Chiang HY, Chen CT, Chien HF, Hsieh ST (2005) Skin denervation, neuropathology, and neuropathic pain in a laser-induced focal neuropathy. Neurobiology of disease 18(1): 40-53.

87. Allen AR (1911) Surgery of experimental lesion of spinal cord equivalent to crush injury of fracture dislocation of spinal column, J Am Med Assoc 57: 878-890.

88. Hao JX, Xu XJ, Aldskogius H, Seiger A, Wiesenfeld Hallin Z (1991) Allodynia-like effects in rat after ischemic spinal cord injury photochemically induced by laser irradiation. Pain 45(2): 175-185.

89. Christensen MD, Everhart AW, Pickelman J, Hulsebosch CE (1996) Mechanical and thermal allodynia in chronic central pain following spinal cord injury. Pain 68(1): 97-107.

90. Hulsebosch CE, Xu GY, Perez-Polo JR, Westlund KN, Taylor CP, et al. (2000) Rodent model of chronic central pain after spinal cord contusion injury and effects of gabapentin. J Neurotrauma 17(12) 1205-1217.

91. Yezierski RP, Liu S, Ruenes GL, Kajander KJ, Brewer KL (1998) Intraspinal injections of the AMPA-metabotropic receptor agonist QUIS resulted in neuronal loss, cavity formation, astrocytic scarring, and a prominent inflammatory reaction. Pain 75 141-155.

92. Anderson TE (1982) A controlled pneumatic technique for experimental spinal cord contusion. J Neurosci. Methods 6(4): 327-333.

93. Siddall PJ, Taylor DA, McClelland JM, Rutkowski SB, Cousins MJ (1999) Pain report and the relationship of pain to physical factors in the first 6 months following spinal cord injury. Pain 81(1-2): 187-197.

94. Siddall PJ, Xu CL, Cousins MJ (1995) Allodynia following traumatic spinal cord injury in the rat. Neuroreport 6(9): 1241-1244.

95. Drew GM, Siddall PJ, Duggan AW (2001) Responses of spinal neurons to cutaneous and dorsal root stimuli in rats with mechanical allodynia after contusive spinal cord injury. Brain Res 893(1-2): 59-69.

96. Genovese T, Esposito E, Mazzon E, et al. (2008) Effect of cyclopentanone prostaglandin 15-deoxy-delta12,14pgj2 on early functional recovery from experimental spinal cord injury. Shock 30(2): 142-152.

97. Fiford RJ, Bilston LE, Waite P, Lu J (2004) A vertebral dislocation model of spinal cord injury in rats. Journal of neurotrauma 21(4): 451-458.

98. Vijayaprakash KM, Sridharan N (2013) An experimental spinal cord injury rat model using customized impact device: A cost-effective approach. Journal of pharmacology pharmacotherapeutics 4(3): 211-213.

99. Bunge MB, Holets VR, Bates ML, Clarke TS, Watson BD (1994) Characterization of photochemically induced spinal cord injury in the rat by light and electron microscopy. Exp Neurol 127(1): 76-93.

100. Basso DM, Beattie MS, Bresnahan JC (1996) Graded histological and locomotor outcomes after spinal cord contusion using the NYU weight drop device versus transection. Exp Neurol 139(2): 244-256.

101. Yezierski RP, Santana M, Park SH, Madsen PW (1993) Neuronal degeneration, and spinal cavitation following intraspinal injections of quisqualic acid in the rat. J Neurotrauma 10(4): 445-456.

102. Madsen PW, Yezierski RP, Holets VR (1994) Syringomyelia: clinical observations and experimental studies. J Neurotrauma 11(3): 241-254.

103. Yezierski RP, Park SH (1993) The mechanosensitivity of spinal sensory neurons following intraspinal injections of quisqualic acid in the rat. Neurosci Lett 157(1): 115-119.

104. Liu XZ, Xu XM, Hu R, et al. (1997) Neuronal and glial apoptosis after traumatic spinal cord injury. J Neurosci. 17(14): 5395-5406.

105. Fairbanks CA, Schreiber KL, Brewer KL, et al. (2000) Agmatine reverses pain induced by inflammation, neuropathy, and spinal cord injury. Proc Natl Acad Sci USA 97(19): 10584-10589.

106. Yezierski RP, Liu S, Ruenes GL, Kajander KJ, Brewer KL (1998) Excitotoxic spinal cord injury: behavioral and morphological characteristics of a central pain model. Pain 75(1): 141-155.

107. Watson BD, Prado R, Dietrich WD, Ginsberg MD, Green BA (1986) Photochemically induced spinal cord injury in the rat. Brain Res 367(1-2): 296-300.

108. Prado R, Dietrich WD, Watson BD, Ginsberg MD, Green BA (1987) Photochemically induced graded spinal cord infarction. Behavioral, electrophysiological, and morphological correlates. J Neurosurg 67 (5): 745-753.

109. Xu XJ, Hao JX, Aldskogius H, Seiger A, Wiesenfeld Hallin Z (1992) Chronic pain-related syndrome in rats after ischemic spinal cord lesion: a possible animal model for pain in patients with spinal cord injury. Pain 48(2): 279-290.

110. Hao JX, Xu XJ, Aldskogius H, Seiger A, Wiesenfeld-Hallin Z (1992) Photochemically induced transient spinal ischemia induces behavioral hypersensitivity to mechanical and cold stimuli, but not to noxious-heat stimuli, in the rat. Exp Neurol 118(2): 187-194.

111. Bunge MB, Holets VR, Bates ML, Clarke TS, Watson BD (1994) Characterization of photochemically induced spinal cord injury in the rat by light and electron microscopy. Experimental neurology 127(1): 76-93.

112. Kim J, Yoon YW, Hong SK, Na HS (2003) Cold and mechanical allodynia in both hind paws and tail following thoracic spinal cord hemisection in rats: time courses and their correlates. Neurosci Lett 343(3): 200-204.

113. Koehler PJ, Endtz LJ (1986) The Brown-Sequard sundrome. Arch Neurol 43 (9): 21-924.

114. Saxena T, Deng B, Hasenwinkel JM, Stelzner D, Chaiken J (2011) Raman spectroscopic investigation of spinal cord injury in a rat model. Journal of biomedical optics 16(2): 027003.

115. McCarthy GM, Skillings JR (1992) Jaw and other orofacial pain in patients receiving vincristine for the treatment of cancer. Oral Surg. Oral Med Oral Pathol 74(3): 299-304.

116. Tanner K, Levine J, Topp K (1998) Microtubule disorientation and axonal swelling in unmyelinated sensory axons during vincristine induced painful neuropathy in rat. J Comp Neurol 395(4): 481-492.

117. Topp KS, Tanner KD, Levine JD (2000) Damage to the cytoskeleton of large diameter sensory neurons and myelinated axons in vincristine induced painful peripheral neuropathy in the rat. J Comp Neurol 424(4): 563-576.

118. Tanner KD, Reichling DB, Levine JD (1998) Nociceptor hyper-responsiveness during vincristine-induced painful peripheral neuropathy in the rat. J Neurosci 18(16): 6480-6491.

119. Gottschalk PG, Dyck PJ, Kiely JM (1968) Vinca alkaloid neuropathy: nerve biopsy studies in rats and in man. Neurology 18((9): 875-882.

120. Aley KO, Reichling DB, Levine JD (1996) Vincristine hyperalgesia in the rat: a model of painful vincristine neuropathy in humans. Neuroscience 73(1): 259-265.

121. Sweitzer SM, Pahl JL, DeLeo JA (2006) Propentofylline attenuates vincristine-induced peripheral neuropathy in the rat. Neurosci Lett 400(3): 258-261.

122. Authier N, Gillet JP, Fialip J, Eschalier A, Coudore F (2003) A new animal model of vincristine-induced nociceptive peripheral neuropathy. Neurotoxicology 24(6): 797-805.

123. Aley KO, Levine JD (2002) Different peripheral mechanisms mediate enhanced nociception in metabolic/toxic and traumatic painful peripheral neuropathies in the rat. Neuroscience 111(2): 389-397.

124. Joseph EK, Levine JD (2003) Sexual dimorphism for protein kinase c epsilon signaling in a rat model of vincristine-induced painful peripheral neuropathy. Neuroscience 119(3): 831-838.

125. Lynch JJ III, Wade CL, Zhong CM, Mikusa JP, Honore P (2004) Attenuation of mechanical allodynia by clinically utilized drugs in a rat chemotherapy-induced neuropathic pain model. Pain 110(1-2):56-63.

126. Siau C, Bennett GJ (2006) Dysregulation of neuronal calcium homeostasis in chemotherapy-evoked painful peripheral neuropathy. Anesth Analg 102(5): 1485-1490.

127. Xiao WH, Bennett GJ (2007) Chemotherapy-evoked neuropathic pain: abnormal spontaneous discharge in A-fiber and C-fiber primary afferent neurons and its suppression by acetyl-Lcarnitine. Pain 135(5): 262-270.

128. Ja'afer FM, Hamdan FB, Mohammed FH (2006) Vincristineinduced neuropathy in rat: electrophysiological and histological study. Exp Brain Res 173(2): 334-345.

129. Norido F, Finesso M, Fiorito C, et al. (1988) General toxicity and peripheral nerve alterations induced by chronic vincristine treatment in the rabbit. Toxicol Appl Pharmacol 93(3): 433-441.

130. Fiori MG, Schiavinato A, Lini E, Nunzi MG (1995) Peripheral neuropathy induced by intravenous administration of vincristine sulfate in the rabbit. An ultra structure studies. Toxicol Pathol 23(3): 248-255.

131. Bardos G, Moricz K, Jaszlits L (2003) BGP-15, a hydroximic acid derivative, protects against cisplatin- or taxol-induced peripheral neuropathy in rats. Toxicol Appl Pharmacol 190: 9-16.

132. Vera G, Chiarlone A, Cabezos PA, Pascual D, Mart´ın MI, et al. (2007) WIN 55,212-2 prevents mechanical allodynia but not alterations in feeding behaviour induced by chronic cisplatin in the rat. Life Sci 81: 468-479.

133. Chaudhry V, Chaudhry M, Crawford TO, Simmons O'Brien E, Griffin JW (2003) Toxic neuropathy in patients with pre-existing neuropathy. Neurology 60: 337-340.

134. Markman M (2003) Toxicities of the platinum antineoplastic agents. Expert Opin Drug Saf 2: 597-607.

135. Koning DP, Neijt JP, Jennekens FGI, Gispen WH (1987) Evaluation of cis-di ammine dichloro platinum (II) (Cisplatin) neurotoxicity in rats. Toxicol. Appl. Pharmacol 89: 81-87.

136. Tredici G, Braga M, Nicolini G (1999) Effect of recombinant human nerve growth factor on cisplatin neurotoxicity in rats. Exp Neurol 159: 551-558.

137. Tredici G, Tredici S, Fabbrica D, Minoia C, Cavaletti G (1998) Experimental cisplatin neuronopathy in rats and the effect of retinoic acid administration. J. Neurooncol 36: 31-40.

138. Boyle FM, Wheeler HR, Shenfield GM (1999) Amelioration of experimental cisplatin and paclitaxel neuropathy with glutamate. J. Neurooncol 41: 107-116.

139. Authier N, Gillet JP, Fialip J, Eschalier A, Coudore F (2003) An animal model of nociceptive peripheral neuropathy following repeated cisplatin injections. Exp Neurol 182: 12- 20.

140. Bianchi R, Gilardini A, Rodriguez Menendez V (2007) Cisplatin-induced peripheral neuropathy: neuroprotection by erythropoietin without affecting tumour growth. Eur J Cancer 43: 710-717.

141. Apfel SC, Arezzo JC, Lipson L, Kessler JA (1992) Nerve growth factor prevents experimental cisplatin neuropathy. Ann Neurol 31: 76-80.

142. Szilvassy J, Sziklai I, Racz T, Horvath P, Rabloczky G, et al. (2000) Impaired bronchomotor responses to field stimulation in guineapigs with cisplatin-induced neuropathy. Eur. J. Pharmacol 403: 259-265.

143. Cavaletti G, Tredici G, Marmiroli P, Petruccioli MG, Barajon I, et al. (1992) Morphometric study of the sensory neuron and peripheral nerve changes induced by chronic cisplatin (DDP) administration in rats. Acta. Neuropathol (Berl) 84: 364-371.

144. Authier N, Fialip J, Eschalier A, Coudore F (2000) Assessment of allodynia and hyperalgesia after cisplatin administration to rats. Neurosci Lett 291: 73-76.

145. Grothey A (2003) Oxaliplatin-safety profile: neurotoxicity. Semin Oncol 30: 5-13.

146. Cersosimo RJ (2005) Oxaliplatin-associated neuropathy: a review.Ann. Pharmacother 39: 128-135.

147. Cavaletti G, Tredici G, Petruccioli MG (2001) Effects of different schedules of oxaliplatin treatment on the peripheral nervous system of the rat. Eur J Cancer 37: 2457- 2463.

148. Jamieson SM, Liu J, Connor B, McKeage MJ (2005) Oxaliplatin causes selective atrophy of a subpopulation of dorsal root ganglion neurons without inducing cell loss. Cancer Chemother. Pharmacol 56: 391-399.

149. Ling B, Authier N, Balayssac D, Eschalier A, Coudore F (2007) Behavioral and pharmacological description of oxaliplatininduced painful neuropathy in rat. Pain 128: 225-234.

150. Ling B, Coudor¢e Civiale MA, Balayssac D, Eschalier A, Coudore F, et al. (2007) Behavioral and immunohistological assessment of painful neuropathy induced by a single oxaliplatin injection in the rat. Toxicology 234: 176-184.

151. Dougherty PM, Cata JP, Cordella JV, Burton A, Weng HR (2004) Taxol induced sensory disturbance is characterized by preferential impairment of myelinated fiber function in cancer patients. Pain 109: 132-142.

152. Kono T, Suzuki Y, Mizuno K, Miyagi C, Omiya Y, (2015) Preventive effect of oral goshajinkigan on chronic oxaliplatin-induced hypoesthesia in rats. Scientific reports 5(1): 1-11.

153. Lee JJ, Swain SM (2006) Peripheral neuropathy induced by microtubule stabilizing agents. J Clin Oncol 24: 1633-1642.

154. Mielke S, Sparreboom A, Mross K (2006) Peripheral neuropathy: a persisting challenge in paclitaxel-based regimes. Eur J Cancer 42: 24-30.

155. Persohn E, Canta A, Schoepfer S (2005) Morphological and morphometric analysis of paclitaxel and docetaxel-induced peripheral neuropathy in rats. Eur J Cancer 41: 1460- 1466.

156. Cavaletti G, Bogliun G, Marzorati L (1995) Peripheral neurotoxicity of taxol in patients previously treated with cisplatin.Cancer 75: 1141-1150.

157. Polomanoa RC, Mannes AJ, Clark US, Bennett GJ (2001) A painful peripheral neuropathy in the rat produced by the chemotherapeutic drug, paclitaxel. Pain 94: 293-304.

158. Flatters SJL, Bennett GJ (2006) Studies of peripheral sensory nerves in paclitaxel-induced painful peripheral neuropathy: evidence for mitochondrial dysfunction. Pain 122: 247-257.

159. Kilpatrick TJ, Phan S, Reardon K, Lopes EC, Cheema SS (2001) Leukaemia inhibitory factor abrogates Paclitaxel-induced axonal atrophy in the Wistar rat. Brain Res. 911: 163- 167.

160. Authier N, Gillet JP, Fialip J, Eschalier A, Coudore F (2000) Description of a short-term Taxol-induced nociceptive neuropathy in rats. Brain Res 887: 239-249.

161. Cliffer KD, Siuciak JA, Carson SR (1998) Physiological characterization of Taxol induced large-fiber sensory neuropathy in the rat. Ann Neurol 43: 46-55.

162. Peters CM, Jimenez-Andrade JM, Jonas BM (2007) Intravenous paclitaxel administration in the rat induces a peripheral sensory neuropathy characterized by macrophage infiltration and injury to sensory neurons and their supporting cells. Exp. Neurol. 203: 42-54.

163. Dina OA, Chen X, Reichling D, Levine JD (2001) Role of protine kinase cepsilon and protine kinase A in a model of paclitaxelinduced painful perioheral neuropathy in the rat. Neuroscience 108: 507-515.

164. Roglio I, Bianchi R, Camozzi F (2009) Docetaxel-induced peripheral neuropathy: protective effects of dihydroprogesterone and progesterone in an experimental model. J Peripher Nerv Syst 14: 36-44.

165. Peng P, X, Q, Xia S, Zhuang L, Gui Q, et al. (2012) Pregabalin attenuates docetaxel-induced neuropathy in rats. Journal of Huazhong University of Science and Technology 32(4): pp.586-590.

166. Pardo CA, McArthur JC, Griffin JW (2001) HIV neuropathy: insights in the pathology of HIV peripheral nerve disease. J. Peripher. Nerv Syst 6: 21-27.

167. Bhangoo SK, Ren D, Miller RJ (2007) CXCR4 chemokine receptor signaling mediates pain hypersensitivity in association with antiretroviral toxic neuropathy. Brain Behav Immun 21: 581-591.

168. Dalakas MC (2001) Peripheral neuropathy and antiretroviral drugs. J Peripher Neurol 6: 14-20.

169. Patterson TA, Schmued LC, Sandberg JA, Slikker W (2000) Temporal development of 2,3-dideoxyinosine (ddI)-induced peripheral myelinopathy. Neurotoxicol. Teratol 22: 429-434.

170. Joseph EK, Chen X, Khasar SG, Levine JD (2004) Novel mechanism of enhanced nociception in a model of AIDS therapyinduced painful peripheral neuropathy in the rat. Pain 107: 147-158.

171. Cooley TP, Kunches LM, Saunders CA (1990) Treatment of AIDS and AIDS-related complex with 2,3 dideoxyinosine given once daily. Rev Infect Dis 12: S552-S560.

172. Calcutt NA (2002) Potential mechanisms of neuropathic pain in diabetes. Int Rev Neurobiol 50: 205-228.

173. Courteix C, Eschalier A, Lavarenne J (1993) Streptozocin induced diabetic rats: behavioural evidence for a model of chronic pain. Pain 53: 81-88.

174. Lee J, Cox D, Mook D, McCarty R (1990) Effect of hyperglycemia on pain threshold in alloxan-diabetic rats. Pain 40: 105- 107.

175. Khan N, Singh N, Jaggi AS (2008) Possible role of spleen-derived factors, vanilloid receptors and calcitonin gene-related peptide in diabetes induced hyperalgesia in mice. Yakugaku Zasshi 128: 1699-1705.

176. Anjaneyulu M, Chopra K (2003) Quercetin A bioflavonoid, attenuates thermal hyperalgesia in a mouse model of diabetic neuropathic pain. Prog. Neuropsychopharmacol. Biol. Psychiatry 27: 1001-1005.

177. Aley KO, Levine JD (2001) Rapid onset pain induced by intravenous Streptozotocin in the rat. J Pain 2: 146-150.

178. Goto Y, Suzuki K, Ono T, Sasaki M, Toyota T (1988) Development of diabetes in the non-obese NIDDM rat (GK rat). Adv. Exp.Med. Biol 246: 29-31.

179. Bisbis S, Bailbe D, Tormo MA (1993) Insulin resistance in the GK rat: decreased receptor number but normal kinase activity in liver. Am. J. Physiol 265: E807-E813.

180. O'Rourke CM, Davis JA, Saltiel AR, Cornicelli JA (1997) Metabolic effects of troglitazone in the Goto-Kakizaki rat, a nonobese and normolipidemic rodent model of non-insulindependent diabetes mellitus. Metabolism 46: 192-198.

181. Ueta K, Ishihara T, Matsumoto Y (2005) Long-term treatment with the Na+-glucose cotransporter inhibitor T-1095 causes sustained improvement in hyperglycemia and prevents diabetic neuropathy in Goto-Kakizaki Rats. Life Sci 76: 2655-2668.

182. Li F, Abatan OI, Kim H (2006) Taurine reverses neurological and neurovascular deficits in Zucker diabetic fatty rats. Neurobiol. Dis 22: 669-676.

183. Murakawa Y, Zhang W, Pierson CR (2002) Impaired glucose tolerance and insulinopenia in the GK-rat causes peripheral neuropathy. Diabetes Metab Res Rev 18: 473-483.

184. Oltman CL, Coppey LJ, Gellett JS, Davidson EP, Lund DD, Yorek MA () Progression of vascular and neural dysfunction in sciatic nerves of Zucker diabetic fatty and Zucker rats. Am J.

185. Sima AA, Kamiya H (2006) Diabetic neuropathy differs in type 1 and type 2 diabetes. Ann N Y Acad Sci 1084: 235- 249.

186. Schmidt RE, Dorsey DA, Beaudet LN, Parvin CA, Zhang W, et al. (2004) Experimental rat models of types 1 and 2diabetes differ in sympathetic neuroaxonal dystrophy. J.Neuropathol. Exp Neurol 63: 450-460.

187. Underwood RA, Gibran NS, Muffley LA, Usui ML, Olerud JE (2001) Color subtractive-computer-assisted image analysis for quantification of cutaneous nerves in a diabetic mouse model. J. Histochem. Cytochem 49: 1285-1291.

188. Norido F, Canella R, Zanoni R, Gorio A (1984) Development of diabetic neuropathy in the C57BL/Ks (db/db) mouse and its treatment with gangliosides. Exp. Neurol 83: 221-232.

189. Coleman DL (1982) Diabetes-obesity syndromes in mice. Diabetes 31(Suppl. 1): 1-6.

190. Houseknecht KL, Portocarrero CP (1998) Leptin and its receptors: regulators of whole-body energy homeostasis. Domest. Anim. Endocrinol 15: 457-475.

191. Drel VR, Mashtalir N, Ilnytska O (2006) The leptin-deficient (ob/ob) mouse: a new animal model of peripheral neuropathy of Type 2 diabetes and obesity. Diabetes 55: 3335- 3343.

192. Muller KA, Ryals JM, Feldman EL, Wright DE (2008) Abnormal muscle spindle innervation and large-fiber neuropathy in diabetic mice. Diabetes 57: 1693-1701.

193. Kamiya H, Murakawa Y, Zhang W, Sima AAF (2005) Unmyelinated fiber sensory neuropathy differs in type 1 and type 2 diabetes. Diabetes Metab Res Rev 21: 448-458.

194. Dyck PJ, Dyck PJ, Larson TS, O'Brien PC, Velosa JA (2000) Patterns of quantitative sensation testing of hypoesthesia and hyperalgesia are predictive of diabetic polyneuropathy: a study of three cohorts: Nerve Growth Factor Study Group. Diabetes Care 23: 510-517.

195. Obrosova IG, Mabley JG, Zsengelle´r Z (2005) Role for nitrosative stress in diabetic neuropathy: evidence from studies with a peroxynitrite decomposition catalyst. FASEB J 19: 401-403.

196. Gabra BH, Sirois P (2005) Hyperalgesia in non-obese diabetic (NOD) mice: a role for the inducible bradykinin B1 receptor. Eur. J. Pharmacol 514: 61-67.

197. Kamiya H, Zhang W, Ekberg K, Wahren J, Sima AA (2006) C-Peptide reverses nociceptive neuropathy in type 1 diabetes. Diabetes 55: 3581-3587.

198. Zhang W, Murakawa Y, Wozniak KM, Slusher B, Sima AA (2006) The preventive and therapeutic effects of GCPII (NAALADase) inhibition on painful and sensory diabetic neuropathy. J Neurol Sci 247: 217-223.

199. Zhang W, Murakawa Y, Wozniak KM, Slusher B, Sima AAF (2002) GCPII (NAALADase) inhibition prevents long-term diabetic neuropathy in type 1 diabetic BB-Wor-rat. J Neurol Sci 194: 21-28.

200. Menendez L, Lastra A, Fresno MF (2003) Initial thermal heat hypoalgesia and delayed hyperalgesia in a murine model of bone cancer pain. Brain Res 969: 102-109.

201. Schwei MJ, Honore P, Rogers SD (1999) Neurochemical and cellular reorganization of the spinal cord in a murine model of bone cancer pain. J. Neurosci 19: 10886-10897.

202. Wacnik PW, Eikmeier LJ, Ruggles TR (2001) Functional interactions between tumor and peripheral nerve: morphology, algogen identification, and behavioral characterization of a new murine model of cancer pain. J Neurosci 21: 9355-9366.

203. Shimoyama M, Tanaka K, Hasue F, Shimoyama N (2002) A mouse model of neuropathic cancer pain. Pain 99: 167-174.

204. Sasamura T, Nakamura S, Iida Y (2002) Morphine analgesia suppresses tumor growth and metastasis in a mouse model of cancer pain produced by orthotopic tumor inoculation. Eur J Pharmacol 441: 185-191.

205. Mantyh PW (2004) A mechanism-based understanding of bone cancer pain. Novartis Found Symp 261: 194-214.

206. Mercadante S (1997) Malignant bone pain: pathophysiology and treatment. Pain 69: 1-18.

207. Mao Ying QL, Zhao J, Dong ZQ, Wang J, Yu J, et al. (2006) A rat model of bone cancer pain induced by intra-tibia inoculation of Walker 256 mammary gland carcinoma cells. Biochemical and biophysical research communications 345(4): 1292-1298.

208. Vermeirsch H, Nuydens R, Salmon P, Meert T (2004) Bone cancer pain model in mice: evaluation of pain behavior, bone destruction and morphine sensitivity. Pharmacol. Biochem. Behav 79: 243-251.

209. Hald A, Nedergaard S, Hansen RR, Ding M, Heegaard AM (2009) Differential activation of spinal cord glial cells in murine models of neuropathic and cancer pain. Eur J Pain 13: 138-145.

210. Niiyama Y, Kawamata T, Yamamoto J, Furuse S, Namiki A (2009) SB366791, a TRPV1 antagonist, potentiates analgesic effects of systemic morphine in a murine model of bone cancer pain.Br J Anaesth 102: 251-258.

211. Honore P, Rogers SD, Schwei MJ (2000) Murine models of inflammatory, neuropathic and cancer pain each generates a unique set of neurochemical changes in the spinal cord and sensory neurons. Neuroscience 98: 585-598.

212. Honore P, Schwei J, Rogers SD (2000) Cellular and neurochemical remodeling of the spinal cord in bone cancer pain. Prog Brain Res 129: 389-397.

213. Khasabova IA, Khasabov SG, Harding Rose C (2009) A decrease in anandamide signaling contributes to the maintenance of cutaneous mechanical hyperalgesia in a model of bone cancer pain. J Neurosci 28: 11141-11152.

214. Cain DM, Wacnik PW, Turner M (2001) Functional interactions between tumor and peripheral nerve: changes in excitability and morphology of primary afferent fibers in a murine model of cancer pain. J Neurosci 21: 9367- 9376.

215. Medhurst SJ, Walker K, Bowes M (2002) A rat model of bone cancer pain. Pain 96: 129-140.

216. Mao Ying QL, Ren DH, Mi WL, Liu Q, Wang YQ (2008) Analgesic effects of electroacupuncture combined with Celebrex on rats with tibial cancer pain 6: 830-835.

217. Wacnik PW, Kehl LJ, Trempe TM, Ramnaraine ML, Beitz AJ, et al. (2003) Tumor implantation in mouse humerus evokes movement-related hyperalgesia exceeding that evoked by intramuscular carrageenan. Pain 101: 175-186.

218. Zhao C, Wacnik PW, Tall JM (2004) Analgesic effects of a soy-containing diet in three murine bone cancer pain models. J. Pain 5: 104-110.

219. Andoh T, Sugiyama K, Fujita M (2008) Pharmacological evaluation of morphine and non-opioid analgesic adjuvants in a mouse model of skin cancer pain. Biol Pharm Bull 31: 520-522.

220. Gao YJ, Cheng JK, Zeng Q, Xu ZZ, Decosterd I, et al. (2009) Selective inhibition of JNK with a peptide inhibitor attenuates pain hypersensitivity and tumor growth in a mouse skin cancer pain model. Experimental neurology 219(1): pp.146-155.

221. Oh SB, Tran PB, Gillard SE, Hurley RW, Hammond DL, Miller RJ (2021) Chemokines and glycoprotein120 produce pain hypersensitivity by directly exciting primary nociceptive neurons. J Neurosci 21: 5027-5035.

222. Melli G, Keswani SC, Fischer A, Chen W, Hoke (2006) A Spatially distinct and functionally independent mechanisms of axonal degeneration in a model of HIV-associated sensory neuropathy. Brain 129 1330-1338.

223. Herzberg U, Sagen J (2001) Peripheral nerve exposure to HIV viral envelope protein gp120 induces neuropathic pain and spinal gliosis. J Neuroimmunol 116: 29-39.

224. Wallace VC, Blackbeard J, Pheby T, et al. (2007) Pharmacological, behavioural and mechanistic analysis of HIV-1 gp120 induced painful neuropathy. Pain 133: 47-63.

225. Kennedy PG, Grinfeld E, Gow JW (1999) Latent Varicella-zoster virus in human dorsal root ganglia. Virol 258: 451- 454.

226. Kennedy PG (2002) Key issues in varicella-zoster virus latency. J Neurovirol 8: 80-84.

227. Dworkin RH, Portenoy RK (1994) Proposed classification of herpes zoster pain. Lancet 343: 1648.

228. Sadzot-Delvaux C, Debrus S, Nikkels A, Piette J, Rentier B (1995) Varicella-zoster virus latecy in the adult rat is a useful model for human latent infection. Neurology 12(suppl 8): S18-S20.

229. Sadzot-Delvaux C, Merville Louis MP, Delree P (1990) An in vivo model of varicella-zoster virus latent infection of dorsal root ganglia. J. Neurosci Res 26: 83-89.

230. Dalziel RG, Bingham S, Sutton D (2004) Allodynia in rats infected with varicella zoster virus - a small animal model for post-herpetic neuralgia. Brain Res Brain Res Rev 46: 234-242.

231. Hasnie FS, Breuer J, Parker S (2007) Further characterization of a rat model of varicella zoster virus-associated pain: relationship between mechanical hypersensitivity and anxietyrelated behavior, and the influence of analgesic drugs. Neuroscience 144: 1495-1508.

232. Krohel GB, Richardson JR, Farrell DF (1976) Herpes simplex neuropathy. Neurology 26: 596-597.

233. Takasaki I, Andoh T, Nitta M, et al. (2000) Pharmacological and immunohistochemical characterization of a mouse model of acute herpetic pain. Jpn J Pharmacol 83: 319-326.

234. Takasaki I, Andoh T, Shiraki K, Kuraishi Y (2000) Allodynia and hyperalgesia induced by herpes simplex virus type-1 infection in mice. Pain 86: 95-101.

235. Pan HL, Khan GM, Alloway KD, Chen SR (2003) Resiniferatoxin induces paradoxical changes in thermal and mechanical sensitivities in rats: mechanism of action. J Neurosci 23: 2911-2919.

236. Chen SR, Pan HL (2005) Effect of systemic and intrathecal gabapentin on allodynia in a new rat model of postherpetic neuralgia. Brain Res 25: 1042-1108.

237. Dina OA, Barletta J, Chen X et al. (2000) Key role for the epsilon isoform of protein kinase C in painful alcoholic neuropathy in the rat. J Neurosci 20: 8614-8619.

238. Dina OA, Messing RO, Levine JD (2006) Ethanol withdrawal induces hyperalgesia mediated by PKCepsilon. Eur J Neurosci 24: 197-204.

239. Lieber CS, DeCarli LM, Sorrell MF (1989) Experimental methods of ethanol administration. Hepatology 10: 501-510.

240. Narita M, Miyoshi K, Narita M, Suzuki T (2007) Involvement of microglia in the ethanol-induced neuropathic pain-like state in the rat. Neurosci Lett 414: 21-25.

241. Miyoshi K, Narita M, Narita M, Suzuki T (2006) Involvement of mGluR5 in the ethanol-induced neuropathic pain-like state in the rat. Neurosci Lett 410: 105-109.

242. Ammendola A, Gemini D, Iannaccone S, et al. (2000) Gender and peripheral neuropathy in chronic alcoholism: a clinical-electroneurographic study. Alcohol Alcohol 35: 368-371.

243. Fu R, Gregor D, Peng Z, Li J, Bekker A, et al. (2015) Chronic intermittent voluntary alcohol drinking induces hyperalgesia in Sprague-Dawley rats. International journal of physiology pathophysiology and pharmacology, 7(3): 136.

244. Hoover DM, Carlton WW, Henrikson CK (1981) Ultrastructural lesions of pyridoxine toxicity in beagle dogs. Vet Pathol 18: 769-777.

245. Schaeppi U, Krinke G (1982) Pyridoxine neuropathy: correlation of functional tests and neuropathology in beagle dogs treated with large doses of vitamin B6. Agents Actions 12: 575-582.

246. Chung JY, Choi JH, Hwang CY, Youn HY (2008) Pyridoxine induced neuropathy by subcutaneous administration in dogs Vet Sci 9: 127-131.

247. Krinke G, Naylor DC, Skorpil V (1985) Pyridoxine megavitaminosis: an analysis of the early changes induced with massive doses of vitamin B6 in rat primary sensory neurons. J Neuropathol Exp Neurol 44: 117-129.

248. Windebank AJ, Low PA, Blexrud MD, Schmelzer JD, Schaumburg HH (1985) Pyridoxine neuropathy in rats: specific degeneration of sensory axons. Neurology 35: 1617- 1622.

249. Krinke GJ, Fitzgerald RE (1988) The pattern of pyridoxine-induced lesion: difference between the high and the low toxic level. Toxicology 49: 171-178.

250. Xu Y, Sladky JT, Brown MJ (1989) Dose-dependent expression of neuronopathy after experimental pyridoxine intoxication. Neurology 39: 1077-1083.

251. Perry TA, Weerasuriya A, Mouton PR, Holloway HW, Greig NH (2004) Pyridoxine-induced toxicity in rats: a stereological quantification of the sensory neuropathy. Exp Neurol 190: 133-144.

252. Krinke G, Naylor DC, Skorpil V (1985) Pyridoxine megavitaminosis: an analysis of the early changes induced with massive doses of vitamin B6 in rat primary sensory neurons. Journal of Neuropathology Experimental Neurology 44(2): 117-129.

253. Kitt CA, Gruber K, Davis M, Woolf CJ, Levine JD (2000) Trigeminal neuralgia: opportunities for research and treatment. Pain 85: 3-7.

254. Love S, Gradidge T, Coakham HB (2001) Trigeminal neuralgia due to multiple sclerosis: ultrastructural findings in trigeminal rhizotomy specimens. Neuropathol Appl Neurobiol 27: 238-244.

255. Osterberg A, Boivie J, Thuomas KA (2005) Central pain in multiple sclerosis - prevalence and clinical characteristics. Eur J Pain 9: 531-542.

256. Ahn DK, Lim EJ, Kim BC, et al. (2008) Compression of the trigeminal ganglion produces prolonged nociceptive behavior in rats. Eup J Pain 13: 568-575.

257. Yang GY, Lee MK, Bae YC, Ahn DK (2009) Intracisternal administration of COX inhibitors attenuate mechanical allodynia following compression of the trigeminal ganglion in rats. Prog. Neuropsychopharmacol Biol Psychiatry 33: 589-595.

258. Imamura Y, Kawamoto H, Nakanishi O (1997) Characterization of heat-hyperalgesia in an experimental trigeminal neuropathy in rats. Exp Brain Res 116: 97-103.

259. Imamura Y, Kawamoto H, Nakanishi O (1997) Characterization of heat-hyperalgesia in an experimental trigeminal neuropathy in rats. Exp Brain Res 116: 97-103.

260. Alvarez P, Dieb W, Hafidi A, Voisin DL, Dallel R (2009) Insular cortex representation of dynamic mechanical allodynia in trigeminal neuropathic rats. Neurobiol Dis 33: 89-95.

261. Eisenberg E, Vos BP, Strassman AM (1996) The peripheral antinociceptive effect of morphine in a rat model of facial pain. Neuroscience 72: 519-525.

262. Ng CH, Ong WY (2001) Increased expression of gamma-aminobutyric acid transporters GAT-1 and GAT-3 in the spinal trigeminal nucleus after facial carrageenan injections. Pain 92: 29-40.

263. Vahidy WH, Ong WY, Farooqui AA, Yeo JF (2006) Effects of intracerebroventricular injections of free fatty acids, lysophospholipids, or platelet activating factor in a mouse model of orofacial pain. Exp Brain Res 174: 781-785.

264. Costa LG, Deng H, Callernan CJ, Bergmark E (1995) Evaluation of the neurotoxicity of glycidamide, an epoxidemetabolite of acrylamide: behavioral, neurochemical, and morphological studies. Toxicology 98: 151-161.

265. Stadler RH, Blank I, Varga N, et al. (2002) Acrylamide from Maillard reaction products. Nature 419: 449-450.

266. Rosen J, Hellenas KE (2002) Analysis of acrylamide in cooked foods by liquid chromatography tandem mass spectrometry. Analyst 127: 880-882.

267. Gold BG, Voda J, Yu X, Gordon H (2004) The immunosuppressant FK506 elicits a neuronal heat shock response and protects against acrylamide neuropathy. Exp Neurol 187: 160-170.

268. Li SX, Cui N, Zhang CL, Zhaoc XL, Yu SF, Xie KQ (2006) Effect of subchronic exposure to acrylamide induced on the expression of bcl-2, bax and caspase-3 in the rat nervous system. Toxicology 217: 46-53.

269. Thakur M, Rahman W, Hobbs C, Dickenson AH, Bennett DL (2012) Characterisation of a peripheral neuropathic component of the rat monoiodoacetate model of osteoarthritis. PloS one 7(3): e33730.

DOI: 10.32474/RRHOAJ.2023.08.000232